

# LOCUS: A Distribution-Free Loss-Quantile Score for Risk-Aware Predictions

Matheus Barreto<sup>1, 2</sup>, Mário de Castro<sup>2</sup>, Thiago R. Ramos<sup>1</sup>, Denis Valle<sup>3</sup>, and Rafael Izbicki<sup>1</sup>

<sup>1</sup>Department of Statistics, Federal University of São Carlos, São Carlos, São Paulo, Brazil

<sup>2</sup>Institute of Mathematics and Computer Science, University of São Paulo, São Carlos, São Paulo, Brazil

<sup>3</sup>School of Forest, Fisheries, and Geomatics Sciences, University of Florida, Gainesville, Florida, United States of America

March 3, 2026

## Abstract

Modern machine learning models can be accurate on average yet still make mistakes that dominate deployment cost. We introduce LOCUS, a distribution-free wrapper that produces a per-input loss-scale reliability score for a fixed prediction function. Rather than quantifying uncertainty about the label, LOCUS models the realized loss of the prediction function using any engine that outputs a predictive distribution for the loss given an input. A simple split-calibration step turns this function into a distribution-free interpretable score that is comparable across inputs and can be read as an upper loss level. The score is useful on its own for ranking, and it can optionally be thresholded to obtain a transparent flagging rule with distribution-free control of large-loss events. Experiments across 13 regression benchmarks show that LOCUS yields effective risk ranking and reduces large-loss frequency compared to standard heuristics.

## 1 Introduction

Modern machine learning models can be highly accurate on average [LeCun et al., 2015, Lakshminarayanan et al., 2017], yet a deployed system is often judged one decision at a time. For a given input  $x$ , the operational question is not only what the model predicts, but whether the prediction is safe to act on or should be flagged for additional review. This need arises across domains such as clinical decision support, credit scoring, and autonomous systems, where rare but large errors dominate the real cost of automation.

A central difficulty is that prediction errors are inherently heterogeneous. Even with abundant data, irreducible (aleatoric) randomness implies that the outcome  $Y$  is not a deterministic function of  $X$  [Kendall and Gal, 2017]. With limited data, (epistemic) uncertainty further amplifies risk in regions where the system has not been well observed [Hüllermeier and Waegeman, 2021]. Consequently, any fixed predictor  $g(x)$  can incur occasional catastrophic losses on inputs that look benign under global performance metrics.

Standard performance summaries such as accuracy, RMSE, ROC curves, and AUC quantify the average performance of a model over the deployment distribution [Fawcett, 2006]. They are useful for model selection and benchmarking, but they are global by construction: they do not tell us how risky a single prediction  $g(x)$  is. Calibration tools such as reliability diagrams, expected calibration error, or conformal prediction sets are important improvements by providing metrics that are more local, yet they still aggregate over many inputs and often do not translate into a simple rule of the form “flag this  $x$  as predictions for it are unreliable”.

In practice, per-instance reliability is usually approximated by some notion of uncertainty. Practitioners estimate the conditional distribution  $Y | X = x$  using Bayesian predictive distributions, deep ensembles, Monte Carlo dropout, prediction intervals or sets, and conformal methods (Lakshminarayanan et al. 2017, Angelopoulos and Bates 2023; see Section 1.2 for related work). These approaches produce quantities such as predictive variances, entropies, or interval widths. A common heuristic is then to flag points with large estimated variability or wide prediction sets, and to trust points with tight predictive distributions. However, these uncertainty proxies are only loosely linked to the quantity that typically matters in deployment: the loss incurred by the prediction that is actually used.

Formally, we fix a deployed prediction function  $g : \mathcal{X} \rightarrow \mathcal{Y}$  and a task loss  $L(\cdot, \cdot)$  (squared error, 0–1 loss, or a domain-specific cost). For a new pair  $(X, Y)$ , we define the realized loss

$$Z = L(g(X), Y).$$

A practitioner typically has a threshold  $\tau$  that encodes *unacceptable error* (e.g., a clinically meaningful deviation). The goal is to design a flagging rule that keeps the event  $\{Z > \tau\}$  rare among predictions we choose to trust, with guarantees that hold in finite samples and without assuming that probabilistic models are correctly specified.

**Our approach: loss-controlled flagging.** We propose LOCUS (LOss Control using Uncertainty Scores), a distribution-free wrapper that turns any estimate of the conditional loss law into a deployable reliability indicator for a fixed prediction function  $g(x)$ . Concretely, given an i.i.d. calibration sample and any black-box engine that outputs a predictive CDF for the realized loss,  $\tilde{F}(\cdot | x) \approx \mathbb{P}(Z \leq \cdot | X = x)$ , we apply a simple split-calibration step to obtain a per-input easily interpretable score  $U_\alpha(x)$ . The resulting  $U_\alpha(x)$  is calibrated on the loss scale and is comparable across inputs. When a loss tolerance  $\tau$  is specified, we accept (do not flag) an input whenever  $U_\alpha(x) \leq \tau$  and flag otherwise, yielding a transparent rule with distribution-free control of large-loss events (Theorem 3).

Figure 1 shows why predictive variance (panel b) can be a poor proxy for deployment risk. For two fixed prediction functions  $g(x)$  (linear, left;  $k$ NN, right), panel (a) plots the data and fitted  $g(x)$ , panel (c) shows the realized loss  $Z = L(g(X), Y)$  together with our loss-scale calibrated upper bound  $U_\alpha(x)$  (an estimated  $(1 - \alpha)$  loss quantile), and panel (d) thresholds  $U_\alpha$  to accept/flag inputs for this specific  $g$ . Interestingly, the linear model incurs a large loss in low-variance regions due to misfit, which  $\sigma(x)$  does not capture, but  $U_\alpha(x)$  does.

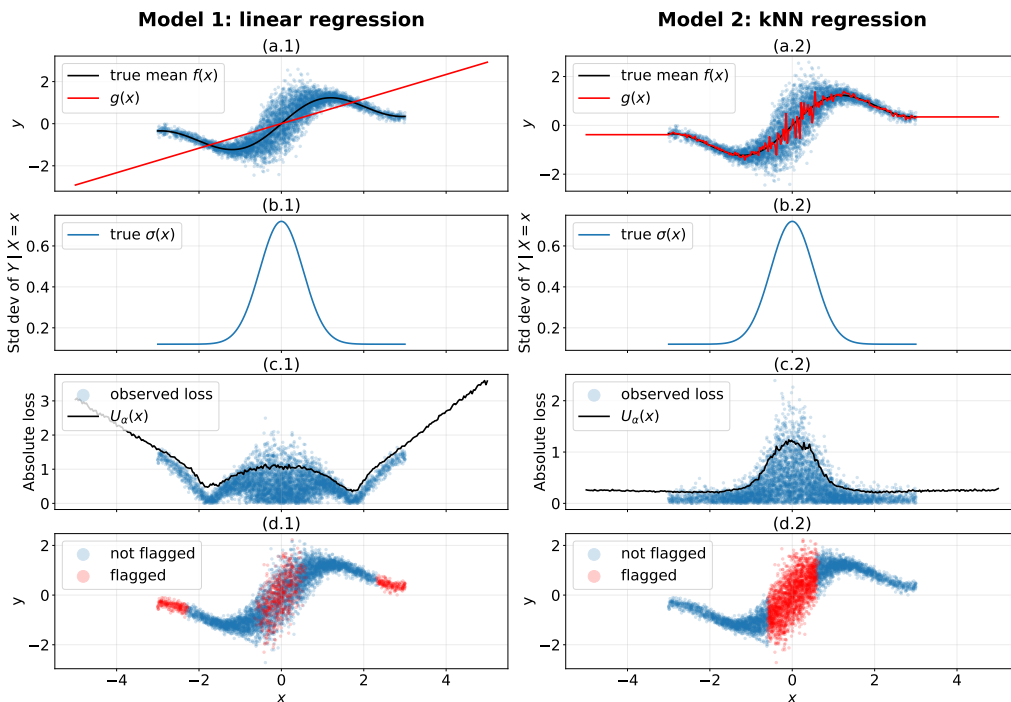


Figure 1: **Loss-centric reliability versus variance.** We fit two models to the same data: linear regression (left) and  $k$ NN regression (right). (a) Data with the true mean  $f(x)$  (black) and fitted prediction function  $g(x)$  (red). (b) True conditional standard deviation  $\sigma(x)$  (aleatoric proxy). (c) Realized absolute loss  $Z = |g(X) - Y|$  (points) and our LOCUS score  $U_\alpha(x)$  (curve), a calibrated estimate of the  $(1 - \alpha)$  loss quantile. (d) The induced accept/flag rule for this specific prediction function: accept if  $U_\alpha(x) \leq \tau$  (blue) and flag otherwise (red).  $U_\alpha$  is interpretable in loss units and captures failures in the predicted values (e.g., linear misfit in low-variance regions) that  $\sigma(x)$  can miss.

## 1.1 Novelty and Contributions

LOCUS is a *loss-centric* reliability wrapper for a fixed prediction function  $g$ , built around the realized loss  $Z = L(g(X), Y)$  rather than uncertainty about  $Y | X = x$ . For flagging, it assumes a user-specified tolerance  $\tau$  on the loss scale, which defines what counts as unacceptable error. We make the following contributions:

- **A calibrated loss-quantile score from any predictive loss CDF.** Given any predictive CDF  $\tilde{F}(\cdot | x)$  for  $Z | X = x$ , we build a local score  $U_\alpha(x)$  with finite-sample, distribution-free marginal validity:

$$\mathbb{P}(Z \leq U_\alpha(X)) \geq 1 - \alpha \quad (\text{Theorem 1}).$$

Under additional assumptions,  $U_\alpha(x)$  also achieves asymptotic conditional validity (Theorem 2), and can be interpreted as a distribution-free calibrated estimate of the upper  $1 - \alpha$  loss quantile at  $x$ : if  $U_\alpha(x) = K$ , then there’s approximately  $\alpha$  probability that the loss at  $x$  will be larger than  $K$ .

- **A simple, interpretable flagging rule with explicit loss control.** Thresholding the bound yields acceptance regions

$$A_{\lambda;\alpha} = \{x : U_\alpha(x) \leq \lambda\}.$$

Setting  $\lambda = \tau$  guarantees distribution-free control of “trusted-but-bad” events:

$$\mathbb{P}(Z > \tau, X \in A_{\tau;\alpha}) \leq \alpha \quad (\text{Theorem 3})$$

This matches the operational objective of bounding the overall frequency of unacceptable losses among predictions we choose to trust. Moreover, we also have that  $\mathbb{P}(Z > \tau \mid X \in A_{\tau;\alpha}) \lesssim \alpha$ , i.e., the probability of a large loss in the accepted samples is approximately smaller than  $\alpha$ .

- **Practical tuning for conditional exceedance targets.** While our core guarantee controls the joint event above, many deployments aim to target a conditional exceedance level  $\eta$  among accepted points,  $\mathbb{P}(Z > \tau \mid X \in A_{\lambda;\alpha}) \approx \eta$ . We provide a simple heuristic validation-based tuning scheme, LOCUS-TUNED, which tunes  $\lambda$  over a grid. We also provide a fully distribution-free validation-based selection of  $\lambda$ , guaranteeing with high probability that  $\mathbb{P}(Z > \tau \mid X \in A_{\lambda^*;\alpha}) \leq \eta$  (Appendix E, Theorem 5).
- **Epistemic-aware inflation without changing calibration.** We introduce default constructions of  $\tilde{F}$  that become more conservative in data-scarce regions, improving robustness in extrapolative regimes while leaving the distribution-free calibration step and guarantees intact.

## 1.2 Relation to Other Work

Our method interacts with three broad lines of work: conformal prediction and risk control, local or conditional coverage methods, and the literature on selective prediction and reject options. Here, we highlight how LOCUS differs from these approaches.

**Selective prediction, reject options, and flagging.** Selective prediction (classification with a reject option) studies rules that either predict or abstain, dating back to Chow’s rule [Chow, 1970] and many cost/coverage variants; see surveys in [Zhang et al., 2023, Hendrickx et al., 2024]. Modern work often learns a selection function (sometimes jointly with a deep predictor) to trade off coverage against performance on the selected subset [Geifman and El-Yaniv, 2017, 2019]. We view LOCUS as a wrapper that induces an acceptance region  $A_{\lambda;\alpha} = \{x : U_\alpha(x) \leq \lambda\}$ , but we do not learn a selector to optimize a coverage–accuracy objective. Instead, we calibrate a per-input upper bound on the realized loss and threshold it to control of large-loss events among accepted cases. The score  $U_\alpha$  is also useful on its own for risk ranking and triage.

As noted by Hendrickx et al. [2024], the literature on reject options for regression is more limited than its classification counterpart. In this context, Zaoui et al. [2020] studies budgeted rejection and obtain variance-thresholding rules, whereas LOCUS targets the realized loss and provides distribution-free loss exceedance control.

**Flagging via uncertainty and OOD scores.** A common way to provide per-instance reliability is to use a scalar *uncertainty proxy* (e.g., predictive variance/entropy, ensemble disagreement) as a triage signal, often obtained from approximate Bayesian methods such as MC dropout or deep ensembles [Gal and Ghahramani, 2016, Lakshminarayanan et al., 2017, Zaoui et al., 2020]. However, such proxies can be misaligned with deployment risk and may fail to increase in regions with few points [Ovadia et al., 2019]. Closely related, *out-of-distribution (OOD) detection* and *open-set recognition* aim to flag atypical inputs using confidence- or distance-based scores (e.g., maximum softmax probability, ODIN, Mahalanobis feature distances) [Hendrycks and Gimpel, 2017, Liang et al., 2018, Lee et al., 2018], with surveys connecting these ideas to anomaly detection and open-set recognition [Geng et al., 2021, Yang et al., 2024]. While effective at detecting atypical inputs, these scores are typically not calibrated to directly control the realized task loss of a fixed deployed predictor on the accepted set. LOCUS instead models the realized loss  $Z = L(g(X), Y)$  and thresholds a calibrated upper loss bound.

**Conformal prediction and risk control.** Classical conformal prediction constructs set-valued predictions with finite-sample marginal coverage under exchangeability [Vovk et al., 2005, Angelopoulos and Bates, 2023, Izbicki, 2025], typically guaranteeing  $\mathbb{P}(Y \in C(X)) \geq 1 - \alpha$  without assumptions on the predictive model. Risk-controlling extensions calibrate prediction sets to bound a user-chosen loss functional aggregated over future points

(e.g., expected risk control) [Bates et al., 2021, Angelopoulos et al., 2024]. These approaches remain global in the sense that they bound an average loss over all future points. In contrast, LOCUS thresholds a loss bound to control catastrophic-loss events on the accepted set via  $\mathbb{P}(Z > \tau, X \in A_{\tau,\alpha}) \leq \alpha$ .

**Local and conditional guarantees.** A growing literature on conformal methods aims to move beyond purely marginal coverage and to provide guarantees that adapt to the local difficulty of the prediction task. Examples include local conformal schemes based on regression trees and forests Cabezas et al. [2024, 2025a,b] and other data-driven groups for local conformal prediction Lei and Wasserman [2014], Izbicki et al. [2020, 2022], Gibbs et al. [2023]. Our method for building  $U_\alpha(x)$  is structurally similar in that it seeks to reflect heterogeneity across  $x$ , but it operates on the distribution of the loss  $Z = L(g(X), Y)$  rather than directly on  $Y$ .

**Epistemic-aware conformal methods.** Recent work has started to explicitly combine aleatoric and epistemic uncertainty within conformal prediction. EPICSCORE introduces a general mechanism for augmenting any conformal score with a Bayesian estimate of epistemic uncertainty, producing prediction regions that automatically widen in data-sparse areas while preserving finite-sample marginal coverage and achieving asymptotic conditional coverage [Cabezas et al., 2025c]. Similarly, LUCCA (Local Uncertainty Conformal Calibration) targets robotics dynamics, calibrating aleatoric uncertainty estimates while accounting for epistemic uncertainty induced by changing environments Marques and Berenson [2024]. LOCUS is complementary: we can use such epistemic-aware calibration to build a sharper, more conservative predictive CDF for  $Z | X = x$ , but the main contribution here is creating an interpretable score to measure reliability of a prediction, plus a flagging layer that turns any predictive CDF for the realized loss into an acceptance rule with explicit guarantees.

## 2 Methodology

Recall the deployed predictor  $g$ , loss  $L$ , and realized loss  $Z = L(g(X), Y)$  (Section 1). Let  $(X, Y)$  denote an independent deployment draw, and let  $D = \{(X_i, Y_i)\}_{i=1}^n$  be an i.i.d. calibration sample from the same deployment distribution, independent of the data used to train  $g$ . Define the observed calibration losses  $Z_i := L(g(X_i), Y_i)$ . Using  $D$ , we construct (i) a calibrated local upper bound  $U_\alpha(x)$  for  $Z | X = x$ , and (ii) flagging rules based on thresholding  $U_\alpha(x)$ .

Our framework has two layers. First, we build a base predictive distribution for the loss  $Z | X = x$  using a probabilistic model fitted on part of the calibration data. Second, we apply a distribution-free calibration step on held-out data to convert the base loss predictive distribution into a valid local upper bound  $U_\alpha(x)$  that satisfies a finite-sample marginal guarantee, regardless of whether the base model is correctly specified. In the next section we detail these steps.

### 2.1 Constructing a calibrated local loss bound

#### Step 1: Data split

We split the calibration sample into two independent parts:

$$D_1 = \{(X_i, Y_i)\}_{i \in I_1} \quad \text{and} \quad D_2 = \{(X_i, Y_i)\}_{i \in I_2},$$

The set  $D_1$  is used to fit a predictive model for  $Z | X$ , while  $D_2$  is used to calibrate. We form the induced loss data

$$\tilde{D}_1 := \{(X_i, Z_i) : i \in I_1\} \quad \text{and} \quad \tilde{D}_2 := \{(X_i, Z_i) : i \in I_2\}.$$

#### Step 2: Base predictive model for $Z | X$

Here we propose two constructions for such a model, though step 3 is agnostic to how step 2 is performed. On  $\tilde{D}_1$  we fit a Bayesian model for  $Z$  given  $X$ . We assume a family of conditional densities

$$\mathcal{F} = \{f(z | x, \theta) : \theta \in \Theta\},$$

modeling the aleatoric variability of  $Z | X = x$ , and place a prior on  $\theta$  ( $\Theta$  can be infinite-dimensional; i.e., this can be a nonparametric model). After observing  $\tilde{D}_1$ , we obtain the posterior  $f(\theta | \tilde{D}_1)$  and the corresponding posterior predictive CDF

$$\begin{aligned} F_Z(z | x, D_1) &:= \mathbb{P}(Z \leq z | x, D_1) \\ &= \int_{\Theta} F_Z(z | x, \theta) f(\theta | \tilde{D}_1) d\theta, \end{aligned} \tag{1}$$

where  $F_Z(z | x, \theta)$  is the CDF induced by  $f(z | x, \theta)$ . Finally, define  $\tilde{F}(\cdot | x) \equiv F_Z(\cdot | x, D_1)$ .

In practice, the posterior may not be computed in closed form. Instead, we can approximate (1) using either Monte Carlo aggregation over posterior draws  $\theta^{(1)}, \dots, \theta^{(S)} \sim f(\theta | \tilde{D}_1)$  (e.g., Bayesian additive regression trees (BART), Monte Carlo dropout, Bayesian neural networks) or a variational approximation (e.g., variational Gaussian processes).

**Alternative definition of  $\tilde{F}$ .** Posterior averaging in (1) may fail to reflect a higher probability of loss in data-scarce or extrapolative regions [Ovadia et al., 2019, Wang et al., 2022]. To explicitly encode epistemic uncertainty, we also define a *density-modulated posterior envelope* for the predictive CDF. Given posterior draws  $\{\theta^{(s)}\}_{s=1}^S$  and a trimming level  $\gamma(x) \in (0, 1)$  (we discuss how to choose it later), define

$$\tilde{F}(z | x) := \text{quantile}_{\gamma(x)}\left(\{F(z | x, \theta^{(s)})\}_{s=1}^S\right). \quad (2)$$

For each fixed  $x$ ,  $\tilde{F}(\cdot | x)$  is a valid CDF in  $z$ . Smaller  $\gamma(x)$  corresponds to a more conservative (lower) envelope of CDFs (heavier right tail), and therefore larger upper bounds.

### Step 3: Distribution-free calibration via PIT values

We calibrate the predictive CDF  $\tilde{F}$  on  $\tilde{D}_2$  using PIT (probability integral transform) values [Zhao et al., 2021, Dey et al., 2025]. For each  $(X_i, Z_i) \in \tilde{D}_2$ , define  $W_i := \tilde{F}(Z_i | X_i)$ . For a target tail level  $\alpha \in (0, 1)$ , define the calibrated level

$$t_{1-\alpha} := \text{quantile}_{1-\alpha}(\{W_i : (X_i, Z_i) \in \tilde{D}_2\}).$$

Finally, define the local performance score as the calibrated upper loss bound

$$U_\alpha(x) := \tilde{F}^{-1}(t_{1-\alpha} | x).$$

**Interpretation of  $U_\alpha(x)$ : conformalized loss quantile.** For a fixed  $\alpha$ , the score  $U_\alpha(x)$  is a local measure of risk: large values signal inputs where the model may incur large loss. It is a calibrated estimate of the  $1 - \alpha$  conditional quantile of the loss at  $x$ .

The calibration step yields a finite-sample marginal guarantee, regardless of whether the base predictive model is correct. Indeed, the next theorem shows that, on a new test point, the realized loss falls below the calibrated bound with probability at least  $1 - \alpha$ , and not far from it.

**Theorem 1** (Marginal validity). *Under the construction above, if the data points are i.i.d.,*

$$\mathbb{P}(Z \leq U_\alpha(X)) \geq 1 - \alpha.$$

*Moreover, if ties between the PIT scores occur with probability 0, then*

$$1 - \alpha + \frac{1}{|\tilde{D}_2| + 1} > \mathbb{P}(Z \leq U_\alpha(X)).$$

Moreover, under additional assumptions that the estimated loss distribution  $\tilde{F}(\cdot | x)$  becomes accurate as the calibration sample grows and that the true conditional loss behavior is well-behaved (see Appendix F),  $U_\alpha$  is approximately the  $1 - \alpha$  quantile of the loss function at  $x$ :

**Theorem 2** (Asymptotic conditional coverage). *Under Assumption 1, we have*

$$\mathbb{P}(Z \leq U_\alpha(x) | X = x, D) \xrightarrow{\mathbb{P}} 1 - \alpha \quad \text{as } n \rightarrow \infty,$$

*where the left-hand side is a random variable (randomness from  $D$ ) and  $\xrightarrow{\mathbb{P}}$  denotes convergence in probability with respect to  $D$ .*

### 2.1.1 Choosing $\gamma(x)$ via kNN radius

To better encode epistemic uncertainty, we let the trimming level  $\gamma(x)$  depend on how well-supported  $x$  is by the design points in  $D_1$ . Intuitively, when  $x$  lies in a data-scarce region, posterior draws for  $Z \mid X = x$  are less reliable, so we choose a smaller  $\gamma(x)$  and take a more conservative lower envelope in (2), which inflates the resulting bound  $U_\alpha(x)$ . Below we give a simple, scalable way to compute such a  $\gamma(x)$  from a local density proxy based on  $k$ -nearest-neighbor distances in a representation space.

Let  $\phi : \mathcal{X} \rightarrow \mathbb{R}^d$  be a representation in which distances are meaningful. For tabular data,  $\phi(x)$  can be standardized covariates. For high-dimensional inputs, we can use an embedding from the predictor  $g$  (e.g. penultimate layer of a neural-network) or from the model used to predict  $Z \mid X$ .

First, we build a nearest neighbor index on  $\{\phi(X_i) : i \in I_1\}$ . Fix  $k$  (e.g.  $k = 50$ ). For any  $x$ , define the kNN radius

$$r_k(x) := \|\phi(x) - \phi(X_{(k)}(x))\|,$$

where  $X_{(k)}(x)$  is the  $k$ -th nearest neighbor of  $x$  among  $\{X_i : i \in I_1\}$ . Larger  $r_k(x)$  indicates lower local design density. Next, compute reference quantiles on  $D_1$  via  $q_{lo} := \text{quantile}_{0.50}(\{r_k(X_i) : i \in I_1\})$  and  $q_{hi} := \text{quantile}_{0.90}(\{r_k(X_i) : i \in I_1\})$ . Now, define the standardized scarcity score

$$s(x) := \frac{r_k(x) - q_{lo}}{q_{hi} - q_{lo} + \varepsilon},$$

for a small value of  $\varepsilon$  (we set it to 0.000001). Then set

$$\gamma(x) = \gamma_{\max} - (\gamma_{\max} - \gamma_{\min}) \cdot \sigma\left(\frac{s(x) - m}{s_\gamma}\right), \quad (3)$$

where  $\sigma$  is the logistic function. We choose  $k = 50$ ,  $\gamma_{\min} = 0.15$ ,  $\gamma_{\max} = 0.9$ ,  $m = 0$ , and  $s_\gamma = 1$ . With this choice,  $\gamma(x)$  is smaller in low-density regions (large  $r_k(x)$ ), yielding a more conservative envelope in (2) and larger bounds  $U_\alpha(x)$ .

## 2.2 Flagging rules based on $U_\alpha(x)$

We now show how to turn the local score  $U_\alpha(x)$  into practical flagging rules that control large losses at the cohort level. Given a threshold  $\lambda \in \mathbb{R}$ , we define the unflagged (accepted) region

$$A_{\lambda;\alpha} := \{x \in \mathcal{X} : U_\alpha(x) \leq \lambda\},$$

and its complement, the flagged region  $A_{\lambda;\alpha}^c := \{x : U_\alpha(x) > \lambda\}$ . We assume the user specifies a tolerance  $\tau$  on the loss scale, which defines what counts as unacceptable error. In what follows, we consider two ways of choosing  $\lambda$ , corresponding to two variants of loss-controlled flagging.

### 2.2.1 Flagging with $\lambda = \tau$

The simplest choice is to set the acceptance threshold equal to the loss threshold,  $\lambda = \tau$ , in which case the acceptance region is  $A_{\tau;\alpha} := \{x : U_\alpha(x) \leq \tau\}$ . In this case we obtain the following guarantee:

**Theorem 3.** *Under the construction above,*

$$\mathbb{P}(Z > \tau, X \in A_{\tau;\alpha}) \leq \alpha.$$

The joint bound controls the overall mass of “trusted but bad” predictions: among all future cases, the fraction that are both unflagged and incur loss above  $\tau$  is at most  $\alpha$ .

Moreover, the next theorem shows that, for large calibration sample sizes, the simple rule “trust the prediction at  $x$  if  $U_\alpha(x) \leq \tau$ ” is approximately equivalent to the oracle rule that would trust  $x$  only when the probability of an unacceptable error at  $x$  is at most  $\alpha$ . That is, thresholding  $U_\alpha$  eventually makes the right flag decision pointwise.

**Theorem 4.** *Fix  $\alpha \in (0, 1)$ , a threshold  $\tau \in \mathbb{R}$ , and a point  $x \in \mathcal{X}$ . Assume that  $F_{Z|X}(\cdot | x)$  is continuous and that its  $(1 - \alpha)$ -quantile  $q_{1-\alpha}(x) := F_{Z|X}^{-1}(1 - \alpha | x)$  is unique. Assume also that  $U_\alpha(x) \xrightarrow{\mathbb{P}} q_{1-\alpha}(x)$  as  $n \rightarrow \infty$  (which holds under the conditions of Theorem 2) and that  $F_{Z|X}(\cdot | x)$  is continuous. Then, the decision rule “accept iff  $U_\alpha(x) \leq \tau$ ” is equivalent to the oracle rule “accept iff  $\mathbb{P}(Z > \tau | X = x) \leq \alpha$ ”.*

Finally, Theorem 2 suggests that  $U_\alpha(x)$  behaves like a  $(1 - \alpha)$  conditional loss quantile, and the selection argument in Theorem 6 (Appendix F) indicates that conditioning on acceptance should preserve this tail level. Hence, we expect the exceedance probability among accepted points to be approximately bounded by  $\alpha$ :

$$\mathbb{P}(Z > \tau \mid X \in A_{\tau;\alpha}) \lesssim \alpha.$$

In words, the accepted set should have an approximately  $\alpha$ -controlled rate of large losses.

### 2.2.2 Locus-Tuned: Tuning $\lambda$

One would often also like the accepted set to satisfy a target *conditional* exceedance level  $\eta$ , namely

$$q(\lambda) := \mathbb{P}(Z > \tau \mid X \in A_{\lambda;\alpha}) \approx \eta.$$

If  $U_\alpha(x)$  were exactly the  $(1 - \alpha)$  conditional quantile of  $Z \mid X = x$ , then choosing  $\alpha = \eta$  and setting  $\lambda = \tau$  would approximately achieve  $q(\tau) \approx \eta$ . In finite samples, however, marginal calibration does not guarantee that the induced accepted set satisfies a desired conditional exceedance rate. When an additional labeled validation set is available, we can tune the acceptance threshold  $\lambda$  to match the target  $\eta$ .

Concretely, let  $D_{\text{val}} = \{(X_i, Y_i)\}_{i=1}^N$  be i.i.d. and independent of the data used to construct  $U_\alpha(\cdot)$ , and define validation losses  $Z_i := L(g(X_i), Y_i)$ . Compute validation scores once,

$$u_i := U_\alpha(X_i), \quad i = 1, \dots, N,$$

and consider a finite grid of thresholds  $\Lambda \subset \mathbb{R}$ . For each  $\lambda \in \Lambda$ , define the accepted index set and its size

$$I_\lambda := \{i : u_i \leq \lambda\}, \quad n_\lambda := |I_\lambda|,$$

and estimate the conditional exceedance rate among accepted validation points by

$$\hat{q}(\lambda) := \frac{1}{n_\lambda \vee 1} \sum_{i \in I_\lambda} \mathbf{1}\{Z_i > \tau\}.$$

A simple selection rule is

$$\hat{\lambda} \in \arg \min_{\lambda \in \Lambda} |\hat{q}(\lambda) - \eta|.$$

In practice, it is often useful to additionally enforce a minimum acceptance constraint (to avoid unstable estimates when  $n_\lambda$  is too small), e.g., restricting to  $\{n_\lambda/N \geq \rho_{\min}\}$ .

This tuning step is heuristic. If one requires a fully distribution-free validation-based choice of  $\lambda$  with a high-probability guarantee that  $\mathbb{P}(Z > \tau \mid X \in A_{\hat{\lambda};\alpha}) \leq \eta$  over a finite grid, see Appendix E. A complementary heuristic that tunes  $\alpha$  while fixing  $\lambda = \tau$  (LOCUS- $\alpha$ ) is provided in the appendix (Section D).

## 3 Experiments

We test our methods on 13 datasets; see Appendix A for a full description. Each dataset is split into train (40%), calibration (40%), validation (10%) and testing (10%) portions. We first train a fixed prediction function  $g$  via a Random Forest [Breiman, 2001]. Using the calibration set, we fit a probabilistic model for the realized loss  $Z = L(g(X), Y)$  and apply the split calibration procedure from Section 2.1 to obtain the calibrated upper loss bound  $U_\alpha(x)$ . We instantiate LOCUS with the following predictive loss distributions  $\tilde{F}(\cdot \mid x)$ : MC-dropout using a mixture density network [Bishop, 1994] and Bayesian additive regression trees [Chipman et al., 2010]. We also present the results for the epistemic-aware  $\gamma(x)$ -inflated variants of these. For simplicity, for each dataset we set the tolerance level  $\tau$  (which defines unacceptable error) so that 30% of the validation observed losses exceed it, i.e., such that  $\mathbb{P}(Z > \tau) \approx 0.3$ . Implementation details are in Appendix B.

### 3.1 $U_\alpha$ and Simple flagging

First, we illustrate why the loss-calibrated score  $U_\alpha$  is more interpretable for per-instance reliability than standard uncertainty proxies, and we also demonstrate the default LOCUS flagger with  $\lambda = \tau$ . We focus on the `homes` dataset (King County house prices). In this experiment we take  $\tau = \$70,000$  as the operational threshold for an

unacceptable absolute error in price, and we estimate  $\tilde{F}$  using MC Dropout. As a reference uncertainty baseline, we also report  $\widehat{sd}(Y | x)$ , an estimate of the conditional standard deviation of the *label* given the features. Details are in Section 3.2 and Appendix B.

Table 1 contrasts  $U_\alpha$  with  $\widehat{sd}(Y | x)$  and an outlier flag from Isolation Forest (baseline OOD detector; Liu et al. [2008]). The key distinction is interpretability on the *loss scale*. While  $\widehat{sd}(Y | x)$  measures dispersion of  $Y | x$ , it does not indicate how large the realized loss  $Z = |g(x) - y|$  can be for that instance, since it does not account for the local quality of the fit of  $g$ . For instance, the third row has a realized absolute error of  $Z \approx \$187,830$ , even though the estimated label variability is only  $\widehat{sd}(Y | x) \approx \$17,150$ ; this illustrates that relatively low dispersion in  $Y | X = x$  can still coincide with a very large loss when  $g$  is locally misaligned. In the same row, the loss-quantile summaries make the risk scale explicit:  $U_{0.5}(x) \approx \$38,640$  suggests a typical error on the order of tens of thousands of dollars, while  $U_{0.1}(x) \approx \$188,920$  indicates that six-figure errors are plausible in the upper tail for that specific input.

Table 1: **Example home-price predictions.** Six test instances from house price predictions; all monetary quantities are in thousands of US dollars. We report  $\hat{y} = g(x)$ ,  $y$ , and  $Z = |\hat{y} - y|$ , alongside LOCUS bounds  $U_{0.5}(x)$  and  $U_{0.1}(x)$  (approx. conditional median and 90th percentile of the loss at each  $x$ ). The LOCUS  $\alpha = 10\%$  flag uses  $\tau = \$70,000$  (flag iff  $U_{0.1}(x) > \tau$ ); IF denotes an Isolation Forest outlier flag;  $\widehat{sd}(Y | X = x)$  is a label-uncertainty baseline.  $U_\alpha(x)$  is interpretable in dollars and can indicate high-loss cases missed by variance or OOD-style scores.

Flagged as unreliable by Locus?	Flagged as outlier by IF?	Outcomes (thousands of US\$)			Locus (thousands of US\$)		Other $\widehat{sd}(Y   X = x)$
		Estimated price $\hat{y}$	True price $y$	$Z =  \hat{y} - y $	$U_{0.5}(x)$	$U_{0.1}(x)$	
yes	yes	2358.64	3567.00	1208.36	294.06	1276.52	104.75
yes	no	1648.52	2200.00	551.48	203.00	554.59	104.07
yes	yes	337.83	150.00	187.83	38.64	188.92	17.15
no	yes	217.85	215.00	2.85	17.94	67.93	76.95
no	yes	208.04	219.95	11.91	17.27	43.58	25.10
no	no	306.03	319.00	12.97	24.87	67.21	31.17

In contrast, the second row shows the complementary failure mode for OOD-style screening: Isolation Forest does not flag the point as an outlier, yet the realized error is  $Z \approx \$551,480$  (predicting \$1,648,520 for a home that sold for \$2,200,000). Here,  $U_{0.5}(x) \approx \$203,000$  and  $U_{0.1}(x) \approx \$554,590$  again communicate directly—on the same dollar scale as the deployment tolerance—that errors well above  $\tau = \$70,000$  are expected for this input. Finally, the bottom block highlights that LOCUS does not flag instances where losses are expected to be small with high probability.

Next, we empirically assess whether the default flagging rule controls the rate of large losses among accepted predictions. Appendix Table 6 reports that, with  $\lambda = \tau$  and  $\alpha = 10\%$ , LOCUS yields conditional exceedance probabilities that are close to the target across nearly all datasets:  $\mathbb{P}(Z > \tau | X \in A_{\tau, \alpha}) \lesssim \alpha$ . In addition, Appendix Table 4 verifies the marginal calibration property: the empirical coverage  $\widehat{\mathbb{P}}(Z \leq U_\alpha(X))$  is consistently at least  $1 - \alpha$ , as expected from Theorem 1. For completeness, we also provide the LOCUS acceptance rate in the Appendix Table 5.

### 3.2 Locus-Tuned

In this section, we compare LOCUS-TUNED—which fixes  $\alpha$  (we use  $\alpha = 10\%$ ) and tunes the acceptance threshold  $\lambda$  on a validation split—to two flagging baselines. (i) **IFlag**: an Isolation Forest anomaly score  $O(x)$ . (ii) **VARNet**: a estimate of label variance,  $V(Y | X = x)$ . Appendix C presents implementation details for VARNet.

Let  $S(x)$  be the score ( $U_\alpha(x)$  for LOCUS,  $\widehat{V}(Y | X = x)$  for VARNet, and  $O(x)$  for IFlag), and define  $A_\lambda := \{x : S(x) \leq \lambda\}$ . For each dataset and method, we choose  $\lambda$  so that  $\widehat{\mathbb{P}}(X \in A_\lambda) \approx 70\%$  on validation, then report  $\mathbb{P}(Z > \tau | X \in A_\lambda)$  on test. With acceptance matched, lower  $\mathbb{P}(Z > \tau | X \in A_\lambda)$  indicates better risk ranking.

Table 2 reports the median of 30 runs for  $\mathbb{P}(Z > \tau | X \in A)$ . across all 13 datasets (with variability measurement in the form of quantiles 5% and 95% in parentheses). The table shows that, at a matched acceptance rate of about 70%, the LOCUS-TUNED scores yield substantially lower conditional large-loss rates than both baselines on every dataset. Isolation-Forest flagging is consistently the weakest, and the label-variance baseline improves on it but

Table 2: **Tuned conditional large-loss rate at matched acceptance.** Conditional exceedance among accepted points,  $\mathbb{P}(Z > \tau \mid X \in A_\lambda)$  (%). For each dataset and method, the threshold  $\lambda$  is selected on the validation split to achieve an acceptance rate of  $\approx 70\%$ ; test performance is then reported. LOCUS-TUNED methods use the LOCUS score  $U_\alpha$  with fixed calibration level  $\alpha = 10\%$ . Entries are the median over 30 runs, with the 5th and 95th percentiles in parentheses; lower is better. Bold marks the lowest value in each row.

Dataset	Baselines (no Locus)		Locus-Tuned (loss-quantile score)			
	IFlag (IF outlier)	VARNet (label var.)	Locus-BART	Locus-BART ( $\gamma$ -infl.)	Locus-MC Dropout	Locus-MC Dropout ( $\gamma$ -infl.)
airfoil	31.0 (27.4; 35.3)	27.5 (23.0; 30.7)	24.7 (19.6; 28.0)	<b>23.1 (18.4; 28.2)</b>	25.0 (18.6; 28.1)	24.3 (19.4; 27.5)
bike	30.1 (30.1; 30.1)	28.4 (26.1; 29.2)	20.1 (19.4; 21.6)	<b>20.0 (19.1; 20.8)</b>	22.6 (21.8; 23.7)	22.9 (21.7; 24.0)
concrete	33.5 (27.2; 38.6)	27.7 (23.0; 31.2)	<b>25.3 (18.7; 29.3)</b>	26.2 (20.5; 30.4)	27.7 (21.5; 31.1)	27.4 (22.7; 32.4)
cycle	28.9 (27.2; 30.0)	29.7 (28.5; 30.2)	<b>27.5 (26.4; 28.6)</b>	28.0 (26.6; 28.8)	28.7 (26.8; 30.4)	29.2 (27.9; 30.1)
electric	31.5 (30.1; 32.1)	29.4 (28.1; 30.7)	24.2 (22.3; 25.4)	<b>24.0 (22.5; 26.2)</b>	24.6 (22.3; 26.4)	24.6 (22.9; 25.8)
homes	34.8 (33.7; 36.0)	26.6 (24.8; 27.7)	<b>18.8 (18.2; 20.2)</b>	19.3 (17.5; 20.2)	19.2 (17.9; 20.3)	19.0 (17.9; 20.3)
meps19	36.4 (35.4; 37.4)	24.8 (21.5; 26.6)	15.7 (14.0; 17.4)	15.7 (13.2; 17.4)	14.3 (12.6; 15.2)	<b>14.0 (12.5; 15.1)</b>
protein	28.0 (27.4; 29.0)	27.4 (25.8; 29.4)	23.9 (22.8; 24.9)	23.9 (23.2; 25.0)	23.6 (22.5; 24.3)	<b>23.5 (22.5; 24.4)</b>
star	29.1 (26.3; 31.9)	29.0 (26.9; 33.8)	29.0 (26.3; 31.7)	28.8 (26.4; 32.2)	<b>28.6 (24.3; 32.4)</b>	29.3 (26.8; 32.5)
superconductivity	24.0 (23.1; 25.3)	25.8 (21.3; 28.1)	18.1 (17.0; 19.7)	<b>18.0 (16.5; 19.5)</b>	18.8 (17.7; 20.9)	18.8 (17.8; 20.3)
wec	34.8 (33.5; 35.3)	23.0 (21.4; 24.6)	15.2 (14.1; 16.6)	14.9 (13.3; 16.0)	8.9 (7.9; 10.3)	<b>8.8 (8.3; 9.8)</b>
winered	30.2 (26.6; 32.9)	28.8 (24.9; 32.9)	26.7 (23.3; 30.8)	<b>26.4 (23.1; 29.7)</b>	27.4 (22.8; 31.5)	27.2 (22.0; 31.1)
winewhite	29.9 (28.2; 31.5)	30.3 (28.3; 31.7)	27.4 (25.8; 29.5)	<b>26.8 (24.5; 29.1)</b>	28.2 (25.5; 29.0)	27.8 (24.9; 29.7)

remains well above the best loss-quantile scores. Among LOCUS-TUNED variants, the winner alternates across datasets: BART (or its  $\gamma$ -inflated version) is strongest on several tabular benchmarks, while MC Dropout with  $\gamma(x)$  inflation often performs best or ties for best.

Table 7 presents the empirical acceptance rates in the test split. We note that the 70% acceptance rate restriction is approximately respected.

Alternatively, it’s possible to tune the  $\alpha$  parameter, which shows similar results to LOCUS-TUNED. Appendix D describes this procedure. Metrics  $P(X \in A)$  and  $P(Z > \tau | X \in A)$  are presented, respectively, in Appendix Tables 8 and 9.

## 4 Final Remarks

LOCUS outputs a single per-input quantity, the calibrated loss score  $U_\alpha(x)$ , on the same scale as the deployed loss  $Z = L(g(X), Y)$ .  $U_\alpha$  is informative *on its own*: it provides an interpretable, decision-relevant risk signal for ranking, triage, and resource allocation, often without committing *a priori* to a fixed accept/reject operating point.

By construction,  $U_\alpha$  satisfies the distribution-free guarantee  $\mathbb{P}(Z \leq U_\alpha(X)) \geq 1 - \alpha$  and, under mild conditions on the base loss model,  $U_\alpha(x)$  converges to the conditional  $(1 - \alpha)$ -quantile of  $Z \mid X = x$ .

When a binary decision is needed, a transparent default accepts when  $U_\alpha(x) \leq \tau$  and guarantees explicit control of “trusted-but-bad” events:  $\mathbb{P}(Z > \tau, U_\alpha(X) \leq \tau) \leq \alpha$  and, approximately,  $\mathbb{P}(Z > \tau \mid X \in A_{\tau; \alpha}) \lesssim \alpha$  (as the experiments corroborate). Alternatively, one may tune  $\alpha$  or  $\lambda$  to control errors inside the accepted set.

Our framework is modular: any engine that outputs a predictive CDF for the realized loss  $Z \mid X = x$  can be used in Step 2 (e.g., normalizing flows [Papamakarios et al., 2021], FlexCode [Izbicki and Lee, 2017], or mixture density networks [Bishop, 1994] or others [Izbicki and Lee, 2016, Dalmaso et al., 2020]), while Step 3 conformalizes it into a valid upper bound. The optional  $\gamma(x)$ -inflated envelope increases conservativeness in data-scarce regions without changing either the calibration step or the finite-sample guarantees. Computationally, once the loss model  $\tilde{F}(\cdot \mid x)$  is fit and the calibration PIT values are computed, varying  $\alpha$  only changes the scalar threshold  $t_{1-\alpha}$ ; the corresponding family  $\{U_\alpha(x)\}_\alpha$  can therefore be obtained with minimal additional overhead, and evaluating  $U_\alpha(x)$  at new inputs is just a CDF inversion.

Although our presentation focuses on regression, LOCUS only assumes a scalar loss is known. It therefore extends naturally to classification and other cost-sensitive problems as long as the task is governed by a single numerical notion of error.

## Acknowledgements

The work of Mario de Castro is partially funded by CNPq, Brazil (grant 301596/2025-5 ). Rafael Izbicki is grateful for the financial support of CNPq (422705/2021-7, 305065/2023-8 and 403458/2025-0) and FAPESP (grant 2023/07068-1). Thiago R. Ramos is grateful for the financial support of CNPq (403458/2025-0). Denis Valle

was partially supported by the US Department of Agriculture National Institute of Food and Agriculture McIntire–Stennis project 1005163 and US National Science Foundation award 2040819.

## References

- AHRQ. Medical expenditure panel survey (meps) 2019 full year consolidated data file (hc-181). [https://meps.ahrq.gov/mepsweb/data\\_stats/download\\_data\\_files\\_detail.jsp?cboPufNumber=HC-181](https://meps.ahrq.gov/mepsweb/data_stats/download_data_files_detail.jsp?cboPufNumber=HC-181), 2019. Accessed: February 2026.
- Anastasios N. Angelopoulos and Stephen Bates. Conformal prediction: A gentle introduction. *Foundations and Trends in Machine Learning*, 16(4):494–591, 2023.
- Anastasios N. Angelopoulos, Stephen Bates, Adam Fisch, Lihua Lei, and Tal Schuster. Conformal risk control. In *International Conference on Learning Representations (ICLR)*, 2024. arXiv:2208.02814.
- Stephen Bates, Anastasios N. Angelopoulos, Lihua Lei, Jitendra Malik, and Michael I. Jordan. Distribution-free, risk-controlling prediction sets. *Journal of the ACM*, 68(6), 2021. doi: 10.1145/3478535. Article 43.
- Christopher M. Bishop. Mixture density networks. Technical Report NCRG/94/004, Neural Computing Research Group, Aston University, Birmingham, UK, February 1994. URL [https://publications.aston.ac.uk/id/eprint/373/1/NCRG\\_94\\_004.pdf](https://publications.aston.ac.uk/id/eprint/373/1/NCRG_94_004.pdf). Previously issued as NCRG/94/4288.
- Leo Breiman. Random forests. *Machine learning*, 45(1):5–32, 2001.
- Luben Cabezas, Guilherme P. Soares, Thiago R. Ramos, Rafael B. Stern, and Rafael Izbicki. Distribution-free calibration of statistical confidence sets. arXiv preprint arXiv:2411.19368, 2024.
- Luben Cabezas, Mateus P. Otto, Rafael Izbicki, and Rafael B. Stern. Regression trees for fast and adaptive prediction intervals. *Information Sciences*, 686, 2025a. Article 121369.
- Luben Cabezas, Vagner S Santos, Thiago R Ramos, Pedro LC Rodrigues, and Rafael Izbicki. Cp4sbi: Local conformal calibration of credible sets in simulation-based inference. *arXiv preprint arXiv:2508.17077*, 2025b.
- Luben Cabezas, Vagner Silva Santos, Thiago Ramos, and Rafael Izbicki. Epistemic uncertainty in conformal scores: A unified approach. In Silvia Chiappa and Sara Magliacane, editors, *Proceedings of the Forty-first Conference on Uncertainty in Artificial Intelligence*, volume 286 of *Proceedings of Machine Learning Research*, pages 443–470. PMLR, 21–25 Jul 2025c. URL <https://proceedings.mlr.press/v286/cruz-cabezas25a.html>.
- Hugh A. Chipman, Edward I. George, and Robert E. McCulloch. Bart: Bayesian additive regression trees. *The Annals of Applied Statistics*, 4(1):266–298, 2010. doi: 10.1214/09-AOAS285.
- C. K. Chow. On optimum recognition error and reject tradeoff. *IEEE Transactions on Information Theory*, 16(1): 41–46, 1970. doi: 10.1109/TIT.1970.1054406.
- Paulo Cortez, A. Cerdeira, F. Almeida, T. Matos, and J. Reis. Wine quality (red wine). UCI Machine Learning Repository, 2009.
- Niccolò Dalmaso, Taylor Pospisil, Ann B Lee, Rafael Izbicki, Peter E Freeman, and Alex I Malz. Conditional density estimation tools in python and r with applications to photometric redshifts and likelihood-free cosmological inference. *Astronomy and Computing*, 30:100362, 2020.
- L. Devroye and G. Lugosi. *Combinatorial Methods in Density Estimation*. Springer Series in Statistics. Springer New York, 2001. ISBN 9780387951171. URL <https://books.google.com.br/books?id=jvT-sUt1HZYC>.
- Biprateep Dey, David Zhao, Brett H Andrews, Jeffrey A Newman, Rafael Izbicki, and Ann B Lee. Towards instance-wise calibration: local amortized diagnostics and reshaping of conditional densities (ladar). *Machine Learning: Science and Technology*, 6(4):045058, 2025.
- Dheeru Dua, Casey Graff, et al. Uci machine learning repository. <http://archive.ics.uci.edu/ml>, 2017. Irvine, CA: University of California, School of Information and Computer Science.
- Tom Fawcett. An introduction to ROC analysis. *Pattern Recognition Letters*, 27(8):861–874, 2006.
- Yarin Gal and Zoubin Ghahramani. Dropout as a Bayesian approximation: Representing model uncertainty in deep learning. In *Proceedings of the 33rd International Conference on Machine Learning (ICML)*, 2016.

- Yonatan Geifman and Ran El-Yaniv. Selective classification for deep neural networks. In *Advances in Neural Information Processing Systems*, volume 30, 2017.
- Yonatan Geifman and Ran El-Yaniv. Selectivenet: A deep neural network with an integrated reject option. In *Proceedings of the 36th International Conference on Machine Learning*, volume 97 of *Proceedings of Machine Learning Research*, pages 2151–2159. PMLR, 2019.
- Chuanxing Geng, Sheng-Jun Huang, and Songcan Chen. Recent advances in open set recognition: A survey. *IEEE Transactions on Pattern Analysis and Machine Intelligence*, 43(10):3614–3631, 2021.
- Isaac Gibbs, Chenyi Cherian, and Emmanuel J. Candès. Conformal prediction with conditional guarantees. arXiv preprint arXiv:2305.12616, 2023.
- Kam Hamidieh. Superconductivity data. UCI Machine Learning Repository, 2018.
- Kilian Hendrickx, Lorenzo Perini, Dries Van der Plas, Wannes Meert, and Jesse Davis. Machine learning with a reject option: A survey. *Machine Learning*, 113(5):3073–3110, 2024.
- Dan Hendrycks and Kevin Gimpel. A baseline for detecting misclassified and out-of-distribution examples in neural networks. In *International Conference on Learning Representations (ICLR)*, 2017. arXiv:1610.02136.
- Eyke Hüllermeier and Willem Waegeman. Aleatoric and epistemic uncertainty in machine learning: An introduction to concepts and methods. *Machine Learning*, 110(3):457–506, 2021.
- Rafael Izbicki. *Machine Learning Beyond Point Predictions: Uncertainty Quantification*. 1st edition, 2025. ISBN 978-65-01-20272-3.
- Rafael Izbicki and Ann B Lee. Nonparametric conditional density estimation in a high-dimensional regression setting. *Journal of Computational and Graphical Statistics*, 25(4):1297–1316, 2016.
- Rafael Izbicki and Ann B. Lee. Converting high-dimensional regression to high-dimensional conditional density estimation. *Electronic Journal of Statistics*, 11(2):2800–2831, 2017. doi: 10.1214/17-EJS1302. URL <https://projecteuclid.org/journals/electronic-journal-of-statistics/volume-11/issue-2/Converting-high-dimensional-regression-to-high-dimensional-conditional-density-estimation/10.1214/17-EJS1302.full>.
- Rafael Izbicki, Gilson Shimizu, and Rafael Stern. Flexible distribution-free conditional predictive bands using density estimators. In *International Conference on Artificial Intelligence and Statistics*, pages 3068–3077. PMLR, 2020.
- Rafael Izbicki, Gilson Shimizu, and Rafael B Stern. Cd-split and hpd-split: Efficient conformal regions in high dimensions. *Journal of Machine Learning Research*, 23(87):1–32, 2022.
- Kaggle. House sales in king county, usa. <https://www.kaggle.com/harlfoxem/housesalesprediction/metadata>, 2016. Accessed: August 2019.
- Alex Kendall and Yarin Gal. What uncertainties do we need in Bayesian deep learning for computer vision? In *Advances in Neural Information Processing Systems*, volume 30, 2017.
- Balaji Lakshminarayanan, Alexander Pritzel, and Charles Blundell. Simple and scalable predictive uncertainty estimation using deep ensembles. In *Advances in Neural Information Processing Systems*, volume 30, 2017.
- Yann LeCun, Yoshua Bengio, and Geoffrey Hinton. Deep learning. *Nature*, 521(7553):436–444, 2015.
- Kimin Lee, Kibok Lee, Honglak Lee, and Jinwoo Shin. A simple unified framework for detecting out-of-distribution samples and adversarial attacks. In *Advances in Neural Information Processing Systems (NeurIPS)*, 2018.
- Jing Lei and Larry Wasserman. Distribution-free prediction bands for non-parametric regression. *Journal of the Royal Statistical Society: Series B (Statistical Methodology)*, 76(1):71–96, 2014.
- Shiyu Liang, Yixuan Li, and R. Srikant. Enhancing the reliability of out-of-distribution image detection in neural networks. In *International Conference on Learning Representations (ICLR)*, 2018.
- Fei Tony Liu, Kai Ming Ting, and Zhi-Hua Zhou. Isolation forest. In *Proceedings of the 2008 IEEE International Conference on Data Mining*, pages 413–422. IEEE, 2008. doi: 10.1109/ICDM.2008.17.

- Luís Marques and Dmitry Berenson. Quantifying aleatoric and epistemic dynamics uncertainty via local conformal calibration. arXiv preprint arXiv:2409.08249, 2024. Also presented at WAFR 2024.
- Raj Mehra. Bike sharing demand - rmsle: 0.3194. <https://www.kaggle.com/code/rajmehra03/bike-sharing-demand-rmsle-0-3194/input?select=train.csv>, 2023. Kaggle. Accessed: February 2026.
- Mehdi Neshat, Bradley Alexander, Nataliia Y. Sergiienko, and Markus Wagner. Optimisation of large wave farms using a multi-strategy evolutionary framework. In *Proceedings of the Genetic and Evolutionary Computation Conference (GECCO)*, pages 1150–1158, 2020.
- Yaniv Ovadia, Emily Fertig, Jie Ren, Zachary Nado, David Sculley, Sebastian Nowozin, Joshua Dillon, Balaji Lakshminarayanan, and Jasper Snoek. Can you trust your model’s uncertainty? evaluating predictive uncertainty under dataset shift. *Advances in Neural Information Processing Systems*, 32, 2019.
- George Papamakarios, Eric Nalisnick, Danilo Jimenez Rezende, Shakir Mohamed, and Balaji Lakshminarayanan. Normalizing flows for probabilistic modeling and inference. *Journal of Machine Learning Research*, 22:1–64, 2021. URL <https://jmlr.org/papers/v22/19-1028.html>.
- Vladimir Vovk, Alex Gammerman, and Glenn Shafer. *Algorithmic Learning in a Random World*. Springer, 2005.
- Meijiang Wang, Jingyu He, and P. Richard Hahn. Local gaussian process extrapolation for bart models with applications to causal inference. arXiv preprint arXiv:2204.10963, 2022. Version 2 (revised Feb 24, 2023).
- Jingkang Yang, Kaiyang Zhou, Yixuan Li, and Ziwei Liu. Generalized out-of-distribution detection: A survey. *International Journal of Computer Vision*, 132:5635–5662, 2024.
- Ahmed Zaoui, Christophe Denis, and Mohamed Hebiri. Regression with reject option and application to knn. In *Advances in Neural Information Processing Systems*, 2020.
- Xu-Yao Zhang, Guo-Sen Xie, Xiuli Li, Tao Mei, and Cheng-Lin Liu. A survey on learning to reject. *Proceedings of the IEEE*, 111(2):185–215, 2023. doi: 10.1109/JPROC.2023.3238024.
- David Zhao, Niccolò Dalmaso, Rafael Izbicki, and Ann B Lee. Diagnostics for conditional density models and bayesian inference algorithms. In *Uncertainty in Artificial Intelligence*, pages 1830–1840. PMLR, 2021.

## A Experimental Details

### A.1 Datasets

We use 13 standard regression datasets commonly used in the conformal prediction literature: `airfoil` [Dua et al., 2017], `bike` [Mehra, 2023], `concrete` [Dua et al., 2017], `cycle` [Dua et al., 2017], `homes` [Kaggle, 2016], `electric` [Dua et al., 2017], `meps19` [AHRQ, 2019], `protein` [Dua et al., 2017], `star` [Mehra, 2023], `superconductivity` [Hamidieh, 2018], `wec` [Neshat et al., 2020], `winered` [Cortez et al., 2009], and `winewhite` [Cortez et al., 2009]. Table 3 summarizes the number of samples and features.

Dataset	$n$	$p$
Airfoil	1503	5
Bike	10885	12
Concrete	1030	8
Cycle	9568	4
Homes	21613	17
Electric	10000	12
Meps19	15781	141
Protein	45730	8
Star	2161	48
Superconductivity	21263	81
WEC	54000	49
WineRed	4898	11
WineWhite	1599	11

Table 3: Dataset summary (sizes and feature counts).

### A.2 Splits and preprocessing

For each dataset, we randomly shuffle the full dataset and split it into **40% train**, **40% calibration**, **10% validation**, and **10% test**. The train split is used *only* to fit the deployed predictor  $g$ . The calibration split is used to build  $U_\alpha(\cdot)$  via the internal split  $D_1/D_2$  (Section 2.1). The validation split is used for the tuned variants (Appendix 3.2). The test split is used only for final reporting.

We standardize features and targets using `StandardScaler` fit on the training split, then apply the same transformation to calibration/validation/test. All reported losses are computed on this standardized scale.

**Bike feature engineering.** For `bike`, we construct time-derived covariates (`hour`, `day`, `month`, `year`) from the timestamp and drop the original `datetime`, `casual`, and `registered` columns, matching the provided scripts.

### A.3 Deployed predictor $g$

We use a Random Forest Regressor as the fixed deployed predictor  $g$  on all datasets, with `n_estimators=300` and otherwise default settings. This predictor is trained only on the training split.

### A.4 Loss and threshold $\tau$

We evaluate realized loss using absolute error on the standardized response:  $Z = |g(X) - Y|$ . Each run defines the unacceptable-loss threshold  $\tau$  (denoted `T` in the code) as the empirical 0.7-quantile of the test losses under  $g$ . This choice yields a comparable tail event across datasets (roughly  $\mathbb{P}(Z > \tau) \approx 0.3$  by construction) and is used solely for benchmarking; in deployment,  $\tau$  would be set by domain requirements.

## A.5 Evaluation metrics

Given a fitted bound  $U_\alpha(\cdot)$  and an acceptance threshold  $\lambda$ , define the acceptance region  $A_{\lambda;\alpha} = \{x : U_\alpha(x) \leq \lambda\}$ . We report:

- **Acceptance rate:**  $p_A = \mathbb{P}(X \in A_{\lambda;\alpha})$ .
- **Marginal tail rate:**  $p_{\text{big } Z} = \mathbb{P}(Z > \tau)$ , fixed as 30% in all examples.
- **Conditional tail rate among accepted:**  $p_{\text{big } Z|A} = \mathbb{P}(Z > \tau \mid X \in A_{\lambda;\alpha})$ .
- **Marginal coverage check:**  $p_{\text{conf}} = \mathbb{P}(Z \leq U_\alpha(X))$  (empirically estimated).

## A.6 Repeated runs and uncertainty reporting

For each dataset, we run 30 repetitions with different random seeds. Our tables report the average metric across runs, and we summarize variability across runs in parentheses (via percentile intervals).

## B Implementation Details for $\tilde{F}(\cdot \mid x)$

This appendix documents the concrete choices used to instantiate the predictive loss CDF  $\tilde{F}(\cdot \mid x)$  in the released code.

### B.1 Shared Locus construction

Given calibration data  $(X_i, Y_i)$ , we compute  $Z_i = |g(X_i) - Y_i|$  and randomly split the calibration set into two equal halves,  $D_1$  and  $D_2$ . A probabilistic loss model is fit on  $(X, Z)$  from  $D_1$  to define a predictive loss distribution, and  $D_2$  is used to compute PIT values and the calibrated level  $t_{1-\alpha}$ , yielding the final bound  $U_\alpha(x) = \tilde{F}^{-1}(t_{1-\alpha} \mid x)$ .

### B.2 MC Dropout via MDN

We use a Mixture Density Network (MDN) to model  $Z \mid X = x$  as a  $K$ -component Gaussian mixture with  $K = 5$ . The MDN has one hidden layer of width 64 and dropout rate 0.4. To obtain an approximate posterior predictive distribution, we perform MC dropout with 500 stochastic forward passes. For each  $x$ , we sample from the resulting mixture to estimate quantiles and PIT values, enabling  $\tilde{F}^{-1}(\cdot \mid x)$  and calibration.

### B.3 BART

We use a heteroskedastic BART model implemented in `pymc-bart` / `pymc`. Concretely, we model (i) a mean function and (ii) a log-scale function using two BART components with  $m = 100$  trees each, and a Gaussian likelihood for  $Z$  given these latent functions. Posterior inference uses four chains and 2000 MCMC draws per chain. Posterior predictive samples of  $Z \mid X = x$  are used to compute quantiles and PIT values.

### B.4 Epistemic-aware $\gamma(x)$ inflation

For the BART and MC Dropout models, we modulate conservativeness via a kNN density proxy computed on  $D_1$  using  $k = 50$  nearest neighbors in standardized feature space. The resulting kNN radius is mapped to a  $\gamma(x) \in (0, 1)$  through a logistic transform; smaller  $\gamma(x)$  in sparse regions yields a more conservative predictive CDF envelope.

Operationally, for each test input  $x$  we form a set of candidate CDF values across posterior draws and take a lower envelope (a small quantile) to obtain an inflated CDF  $\tilde{F}(\cdot \mid x)$ . Inversion for  $\tilde{F}^{-1}$  is performed numerically via a bisection procedure.

## C Implementation details for VARNet

In order to provide a estimative for  $V(Y|X)$  we fit two neural networks with two 64 neuron layers and a single neuron output to predict  $E(Y^2 | X = x)$  and  $E^2(Y | X = x)$ . We then take

$$\widehat{V}(Y | X = x) = \widehat{E}(Y^2 | X = x) - \widehat{E}^2(Y | X = x),$$

as a moment estimative of  $V(Y|X = x)$ . The PyTorch library was used in the implementation. The optimized loss function chosen is the mean absolute error (MAE).

## D Alpha tuning with $\lambda = \tau$ (Locus- $\alpha$ )

This appendix describes a simple heuristic for tuning the calibration level  $\alpha$  when one wishes to keep the operational threshold fixed at  $\lambda = \tau$ , i.e., to accept whenever  $U_\alpha(x) \leq \tau$ . The motivation is to target a desired conditional exceedance level  $\eta$  among accepted points:

$$\mathbb{P}(Z > \tau | X \in A_{\tau;\alpha}) \approx \eta, \quad A_{\tau;\alpha} = \{x : U_\alpha(x) \leq \tau\}.$$

Let  $D_{\text{val}} = \{(X_i, Y_i)\}_{i=1}^N$  be an additional labeled validation set, i.i.d. and independent of the calibration data used to construct  $U_\alpha(\cdot)$ . Define validation losses  $Z_i := L(g(X_i), Y_i)$ . Fix a finite grid of candidate levels  $\Gamma \subset (0, 1)$ . For each  $\alpha \in \Gamma$ , compute the corresponding bound  $U_\alpha(\cdot)$  and validation scores

$$u_i(\alpha) := U_\alpha(X_i), \quad i = 1, \dots, N,$$

then define the accepted indices and their count

$$I_\alpha := \{i : u_i(\alpha) \leq \tau\}, \quad n_\alpha := |I_\alpha|.$$

Estimate the conditional exceedance rate among accepted validation points by

$$\widehat{q}(\alpha) := \frac{1}{n_\alpha \vee 1} \sum_{i \in I_\alpha} \mathbf{1}\{Z_i > \tau\}.$$

A basic selection rule is

$$\widehat{\alpha} \in \arg \min_{\alpha \in \Gamma} |\widehat{q}(\alpha) - \eta|.$$

As with  $\lambda$ -tuning, it is often useful to impose a minimum acceptance constraint, e.g., restrict to  $\{\alpha \in \Gamma : n_\alpha/N \geq \rho_{\min}\}$ .

**Computation note.** Once  $\widetilde{F}(\cdot | x)$  is fit on  $D_1$ , the PIT values  $W_i = \widetilde{F}(Z_i | X_i)$  on  $D_2$  can be computed once; changing  $\alpha$  only changes the empirical quantile level  $t_{1-\alpha}$  and therefore the final bound  $U_\alpha(x) = \widetilde{F}^{-1}(t_{1-\alpha} | x)$ . Thus, scanning  $\alpha$  mainly amounts to reusing the same PIT values and recomputing the threshold  $t_{1-\alpha}$ .

**Guarantee.** For any *fixed* (pre-specified)  $\alpha$ , LOCUS- $\tau$  with  $\lambda = \tau$  retains the distribution-free joint tail guarantee  $\mathbb{P}(Z > \tau, X \in A_{\tau;\alpha}) \leq \alpha$  (Theorem 3). The data-driven choice  $\widehat{\alpha}$  above is a practical heuristic and is reported as such.

## E Distribution-free alternatives to Locus-Tuned

To complement the heuristic tuning of  $\lambda$  in LOCUS-TUNED, we provide a fully distribution-free way to choose  $\lambda$  using the validation sample. The goal is to guarantee, with high probability over the randomness in the calibration and validation data, that the conditional exceedance rate among accepted predictions does not exceed a target  $\eta$ :

$$\mathbb{P}(Z > \tau | X \in A_{\lambda;\alpha}) \leq \eta,$$

where  $A_{\lambda;\alpha} := \{x : U_\alpha(x) \leq \lambda\}$ . We consider a data-driven choice  $\lambda^*$  obtained by scanning a finite grid  $\Lambda$  and enforcing the constraint via a simultaneous upper confidence certificate for the ratio

$$q(\lambda) = \mathbb{P}(Z > \tau | X \in A_{\lambda;\alpha}) = \frac{H(\lambda)}{G(\lambda)},$$

where

$$G(\lambda) := \mathbb{P}(X \in A_{\lambda;\alpha}), \quad H(\lambda) := \mathbb{P}(Z > \tau, X \in A_{\lambda;\alpha}).$$

Using uniform finite-sample deviation bounds for the empirical numerator and denominator over  $\Lambda$ , we construct an empirical upper certificate of the form

$$\bar{q}(\lambda) := \frac{\widehat{H}_N(\lambda) + \varepsilon_H}{\widehat{G}_N(\lambda) - \varepsilon_G},$$

and define  $\lambda^*$  as the largest threshold in  $\Lambda$  satisfying  $\bar{q}(\lambda) \leq \eta$  (with the additional requirement  $\widehat{G}_N(\lambda) > \varepsilon_G$  so that the denominator is positive). If no such threshold exists, we use the convention that  $A_{\lambda^*;\alpha} = \emptyset$ .

The next theorem shows that this choice of  $\lambda^*$  yields a distribution-free, finite-sample guarantee: with probability at least  $1 - \delta$  over  $(D, D_{\text{val}})$ , the conditional exceedance probability among accepted points is at most  $\eta$ .

**Theorem 5.** Fix  $\alpha \in (0, 1)$  and let  $U_\alpha$  be constructed from an independent calibration dataset  $D$ . Let  $D_{\text{val}} = \{(X_i, Y_i)\}_{i=1}^N$  be an additional i.i.d. validation sample, independent of  $D$ , and write  $Z_i = L(g(X_i), Y_i)$  and  $u_i = U_\alpha(X_i)$ . Fix  $\tau \in \mathbb{R}$  and a finite set of candidate thresholds  $\Lambda$ .

For  $\lambda \in \Lambda$ , let

$$G(\lambda) := \mathbb{P}(X \in A_{\lambda;\alpha}) = \mathbb{P}(u \leq \lambda), \quad H(\lambda) := \mathbb{P}(Z > \tau, X \in A_{\lambda;\alpha}) = \mathbb{P}(Z > \tau, u \leq \lambda),$$

and, whenever  $G(\lambda) > 0$ ,

$$q(\lambda) := \mathbb{P}(Z > \tau \mid X \in A_{\lambda;\alpha}) = \frac{H(\lambda)}{G(\lambda)}.$$

Also let

$$\widehat{G}_N(\lambda) := \frac{1}{N} \sum_{i=1}^N \mathbf{1}\{u_i \leq \lambda\}, \quad \widehat{H}_N(\lambda) := \frac{1}{N} \sum_{i=1}^N \mathbf{1}\{u_i \leq \lambda\} \mathbf{1}\{Z_i > \tau\}.$$

Fix  $\delta \in (0, 1)$  and  $\eta \in (0, 1)$ , and set

$$\varepsilon_H := 2\sqrt{\frac{\log(2(N+1))}{N}} + \sqrt{\frac{\log(4/\delta)}{2N}}, \quad \varepsilon_G := \sqrt{\frac{\log(4/\delta)}{2N}}.$$

For  $\lambda \in \Lambda$  with  $\widehat{G}_N(\lambda) > \varepsilon_G$ , set

$$\bar{q}(\lambda) := \frac{\widehat{H}_N(\lambda) + \varepsilon_H}{\widehat{G}_N(\lambda) - \varepsilon_G}.$$

Let

$$\mathcal{F} := \left\{ \lambda \in \Lambda : \widehat{G}_N(\lambda) > \varepsilon_G \text{ and } \bar{q}(\lambda) \leq \eta \right\},$$

and choose  $\lambda^* := \max \mathcal{F}$ , with the convention that if  $\mathcal{F} = \emptyset$ , then  $\lambda^*$  is chosen so that  $A_{\lambda^*;\alpha} = \emptyset$ .

Then, with probability at least  $1 - \delta$  over the randomness in  $(D, D_{\text{val}})$ ,

$$\mathbb{P}(Z > \tau \mid X \in A_{\lambda^*;\alpha}) \leq \eta,$$

where the inner probability is with respect to an independent test draw  $(X, Y)$  from the deployment distribution, and we adopt the convention that the left-hand side equals 0 if  $\mathbb{P}(X \in A_{\lambda^*;\alpha}) = 0$ .

## F Proofs and Additional Theorems

*Proof of Theorem 1.* Let  $n_2 := |I_2|$  and define, for an independent test pair  $(X, Y)$  with  $Z = L(g(X), Y)$ ,

$$W_{n_2+1} := \widetilde{F}(Z \mid X), \quad W_i := \widetilde{F}(Z_i \mid X_i) \quad (i \in I_2).$$

Conditional on  $D_1$ , the variables  $W_1, \dots, W_{n_2}, W_{n_2+1}$  are i.i.d. (hence exchangeable). Let  $W_{(1)} \leq \dots \leq W_{(n_2)}$  be the order statistics of  $\{W_i : i \in I_2\}$  and let

$$k := \lceil (1 - \alpha)(n_2 + 1) \rceil, \quad t_{1-\alpha} := \begin{cases} W_{(k)}, & k \leq n_2, \\ 1, & k = n_2 + 1, \end{cases}$$

which is the usual split-conformal empirical  $(1 - \alpha)$ -quantile. By exchangeability,

$$\mathbb{P}(W_{n_2+1} \leq t_{1-\alpha} \mid D_1) \geq \frac{k}{n_2 + 1} \geq 1 - \alpha.$$

Since for each  $x$  the map  $z \mapsto \tilde{F}(z \mid x)$  is nondecreasing,  $W_{n_2+1} \leq t_{1-\alpha}$  is equivalent to

$$Z \leq \tilde{F}^{-1}(t_{1-\alpha} \mid X) = U_\alpha(X).$$

Taking expectations over  $D_1$  yields  $\mathbb{P}(Z \leq U_\alpha(X)) \geq 1 - \alpha$ .

Now, to prove the second part of the theorem, let the rank of  $W_{n_2+1}$  among  $W_1, \dots, W_{n_2}, W_{n_2+1}$  be  $R := 1 + \sum_{i \in I_2} \mathbf{1}\{W_i < W_{n_2+1}\}$ . By exchangeability and the no-ties assumption,  $R$  is uniform on  $\{1, \dots, n_2 + 1\}$ , so

$$\mathbb{P}(R \leq k \mid D_1) = \frac{k}{n_2 + 1}.$$

Moreover, when  $k \leq n_2$  we have  $t_{1-\alpha} = W_{(k)}$  and no ties imply

$$\{W_{n_2+1} \leq t_{1-\alpha}\} = \{W_{n_2+1} \leq W_{(k)}\} = \{R \leq k\},$$

while if  $k = n_2 + 1$  then  $t_{1-\alpha} = 1$  and the same identity holds trivially. Hence, in all cases,

$$\mathbb{P}(W_{n_2+1} \leq t_{1-\alpha} \mid D_1) = \frac{k}{n_2 + 1}.$$

Using again monotonicity of  $z \mapsto \tilde{F}(z \mid x)$ , this yields

$$\mathbb{P}(Z \leq U_\alpha(X) \mid D_1) = \frac{k}{n_2 + 1}.$$

Finally, since  $k = \lceil (1 - \alpha)(n_2 + 1) \rceil$ , we have  $k < (1 - \alpha)(n_2 + 1) + 1$ , and therefore

$$\mathbb{P}(Z \leq U_\alpha(X) \mid D_1) = \frac{k}{n_2 + 1} < 1 - \alpha + \frac{1}{n_2 + 1}.$$

Taking expectations over  $D_1$  gives  $\mathbb{P}(Z \leq U_\alpha(X)) < 1 - \alpha + \frac{1}{n_2 + 1}$ , proving the claimed upper bound.  $\square$

*Proof of Theorem 3.* On  $\{X \in A_{\tau;\alpha}\}$  we have  $U_\alpha(X) \leq \tau$ , hence

$$\{Z > \tau, X \in A_{\tau;\alpha}\} \subseteq \{Z > U_\alpha(X)\}.$$

By Theorem 1,  $\mathbb{P}(Z > U_\alpha(X)) \leq \alpha$ , proving  $\mathbb{P}(Z > \tau, X \in A_{\tau;\alpha}) \leq \alpha$ .  $\square$

**Assumption 1** (Conditions for asymptotic conditional coverage). *Consider a sequence indexed by the total calibration size  $n = |D|$ , with split sizes  $n_1 := |D_1| \rightarrow \infty$  and  $n_2 := |D_2| \rightarrow \infty$  as  $n \rightarrow \infty$ . Let  $\tilde{F}_{n_1}(\cdot \mid x)$  denote the predictive CDF constructed from  $D_1$  (this is  $\tilde{F}(\cdot \mid x)$  in the main text, with dependence on  $n_1$  made explicit). Assume:*

(A1) **Random-design uniform consistency (in probability).** *For an independent deployment draw  $(X, Z)$  (independent of  $D_1$ ), define*

$$\Delta_{n_1} := \sup_{z \in \mathbb{R}} |\tilde{F}_{n_1}(z \mid X) - F_{Z|X}(z \mid X)|.$$

Then,

$$\Delta_{n_1} \xrightarrow{\mathbb{P}} 0 \quad (n_1 \rightarrow \infty),$$

where  $\xrightarrow{\mathbb{P}}$  denotes convergence in probability with respect to the randomness in  $D_1$  and the independent draw  $X$ .

(A2) **Pointwise uniform consistency at the target  $x$  (in probability).** *For the fixed  $x \in \mathcal{X}$  under consideration,*

$$\sup_{z \in \mathbb{R}} |\tilde{F}_{n_1}(z \mid x) - F_{Z|X}(z \mid x)| \xrightarrow{\mathbb{P}} 0 \quad (n_1 \rightarrow \infty),$$

where the probability is over the randomness in  $D_1$ .

(A3) **Regularity of the true conditional law and at the target  $x$ .** (i) For  $P_X$ -almost every  $x'$ , the true conditional CDF  $F_{Z|X}(\cdot | x')$  is continuous. (ii) At the fixed  $x \in \mathcal{X}$  under consideration,  $F_{Z|X}(\cdot | x)$  is continuous and its  $(1 - \alpha)$ -quantile  $q_{1-\alpha}(x) := F_{Z|X}^{-1}(1 - \alpha | x)$  is unique.

*Proof of Theorem 2.* Fix  $x \in \mathcal{X}$  as in the theorem. We prove the result in four steps.

**Step 1: PIT values are asymptotically uniform, and their conditional CDF converges to the identity.** Let  $(X, Z)$  be an independent deployment draw, independent of  $D_1$ . Define the oracle PIT value

$$V := F_{Z|X}(Z | X).$$

Under Assumption 1(A3)(i), for  $P_X$ -almost every  $x'$  the conditional CDF  $F_{Z|X}(\cdot | x')$  is continuous, hence the probability integral transform yields

$$V \sim \text{Unif}(0, 1).$$

Define the estimated PIT value

$$W := \tilde{F}_{n_1}(Z | X).$$

By Assumption 1(A1),

$$|W - V| = |\tilde{F}_{n_1}(Z | X) - F_{Z|X}(Z | X)| \leq \sup_{z \in \mathbb{R}} |\tilde{F}_{n_1}(z | X) - F_{Z|X}(z | X)| = \Delta_{n_1} \xrightarrow{\mathbb{P}} 0.$$

Hence  $W - V \xrightarrow{\mathbb{P}} 0$ , and since  $V \sim \text{Unif}(0, 1)$ , Slutsky's theorem implies

$$W \xrightarrow{\text{Dist}} \text{Unif}(0, 1).$$

We also need a uniform control of the *conditional* CDF of  $W$  given  $D_1$ . Let

$$H_{n_1}(w) := \mathbb{P}(W \leq w | D_1), \quad w \in [0, 1].$$

Fix  $\delta \in (0, 1)$ . Using the inclusions

$$\{V \leq w - \delta\} \subseteq \{W \leq w\} \cup \{|W - V| > \delta\}, \quad \{W \leq w\} \subseteq \{V \leq w + \delta\} \cup \{|W - V| > \delta\},$$

we obtain, for all  $w \in [0, 1]$ ,

$$w - \delta - \mathbb{P}(|W - V| > \delta | D_1) \leq H_{n_1}(w) \leq w + \delta + \mathbb{P}(|W - V| > \delta | D_1).$$

Therefore,

$$\sup_{w \in [0, 1]} |H_{n_1}(w) - w| \leq \delta + \mathbb{P}(|W - V| > \delta | D_1). \quad (4)$$

It remains to show that  $\mathbb{P}(|W - V| > \delta | D_1) \xrightarrow{\mathbb{P}} 0$ . Since  $|W - V| \leq \Delta_{n_1}$ , we have

$$\mathbb{P}(|W - V| > \delta | D_1) \leq \mathbb{P}(\Delta_{n_1} > \delta | D_1).$$

Moreover, Assumption 1(A1) implies  $\mathbb{P}(\Delta_{n_1} > \delta) \rightarrow 0$ . Then for any  $\varepsilon > 0$ , Markov's inequality yields

$$\mathbb{P}(\mathbb{P}(\Delta_{n_1} > \delta | D_1) > \varepsilon) \leq \frac{\mathbb{E}[\mathbb{P}(\Delta_{n_1} > \delta | D_1)]}{\varepsilon} = \frac{\mathbb{P}(\Delta_{n_1} > \delta)}{\varepsilon} \rightarrow 0,$$

so  $\mathbb{P}(\Delta_{n_1} > \delta | D_1) \xrightarrow{\mathbb{P}} 0$ , and hence also  $\mathbb{P}(|W - V| > \delta | D_1) \xrightarrow{\mathbb{P}} 0$ .

Plugging this into (4) and then letting  $\delta \downarrow 0$  gives

$$\sup_{w \in [0, 1]} |H_{n_1}(w) - w| \xrightarrow{\mathbb{P}} 0. \quad (5)$$

**Step 2: The empirical PIT quantile converges to  $1 - \alpha$ .** Conditional on  $D_1$ , the points in  $D_2$  are i.i.d. and independent of  $D_1$ , so  $\{W_{i,n}\}_{i \in I_2}$  are i.i.d. with CDF  $H_{n_1}$ . By the Glivenko–Cantelli theorem (applied conditionally on  $D_1$ ),

$$\sup_{w \in [0, 1]} |\hat{H}_{n_2}(w) - H_{n_1}(w)| \xrightarrow{\text{a.s.}} 0 \quad (n_2 \rightarrow \infty),$$

almost surely in the randomness of  $D_2$  conditional on  $D_1$ . Combining with (5) and the triangle inequality gives

$$\sup_{w \in [0,1]} |\widehat{H}_{n_2}(w) - w| \xrightarrow{\mathbb{P}} 0.$$

We now use continuity of the quantile functional at the uniform CDF. Since the limit CDF  $w \mapsto w$  is continuous and strictly increasing, uniform convergence of CDFs implies convergence of generalized inverses, hence

$$t_{1-\alpha,n} = \widehat{H}_{n_2}^{-1}(1-\alpha) \xrightarrow{\mathbb{P}} 1-\alpha.$$

**Step 3:  $U_{\alpha,n}(x)$  converges to the oracle quantile.** Let  $q_{1-\alpha}(x) := F_{Z|X}^{-1}(1-\alpha | x)$ , unique by Assumption 1(A3). By Assumption 1(A2),

$$\sup_{z \in \mathbb{R}} |\widetilde{F}_{n_1}(z | x) - F_{Z|X}(z | x)| \xrightarrow{\mathbb{P}} 0,$$

and Step 2 gives  $t_{1-\alpha,n} \xrightarrow{\mathbb{P}} 1-\alpha$ . By the same quantile-map continuity argument used in Step 2 (here using the strict increase/continuity at the target quantile from Assumption 1(A3)), it follows that

$$U_{\alpha,n}(x) = \widetilde{F}_{n_1}^{-1}(t_{1-\alpha,n} | x) \xrightarrow{\mathbb{P}} F_{Z|X}^{-1}(1-\alpha | x) = q_{1-\alpha}(x).$$

**Step 4: Conditional coverage convergence.** Because  $D$  is independent of the test point, conditioning on  $D$  and  $X = x$  gives

$$\mathbb{P}(Z \leq U_{\alpha,n}(x) | X = x, D) = F_{Z|X}(U_{\alpha,n}(x) | x).$$

By Step 3,  $U_{\alpha,n}(x) \xrightarrow{\mathbb{P}} q_{1-\alpha}(x)$ . Since  $u \mapsto F_{Z|X}(u | x)$  is continuous at  $q_{1-\alpha}(x)$  (Assumption 1(A3)), the continuous mapping theorem yields

$$F_{Z|X}(U_{\alpha,n}(x) | x) \xrightarrow{\mathbb{P}} F_{Z|X}(q_{1-\alpha}(x) | x) = 1-\alpha.$$

This proves the first displayed convergence in the theorem. □

Finally, we prove Theorem 5.

*Proof of Theorem 5.* Let

$$G(\lambda) := \mathbb{P}(X \in A_{\lambda;\alpha}) = \mathbb{P}(u \leq \lambda), \quad H(\lambda) := \mathbb{P}(Z > \tau, X \in A_{\lambda;\alpha}) = \mathbb{P}(Z > \tau, u \leq \lambda),$$

so that for  $G(\lambda) > 0$ ,

$$q(\lambda) := \mathbb{P}(Z > \tau | X \in A_{\lambda;\alpha}) = \frac{H(\lambda)}{G(\lambda)}.$$

**Step 1: VC-type uniform deviation for the numerator.** Define

$$\Delta_H := \sup_{\lambda \in \Lambda} |\widehat{H}_N(\lambda) - H(\lambda)|.$$

Since changing one observation  $(X_i, Z_i)$  changes each summand  $A_i^\lambda B_i \in \{0, 1\}$  by at most 1, it changes  $\widehat{H}_N(\lambda)$  by at most  $1/N$  for every  $\lambda$ , hence changes  $\Delta_H$  by at most  $1/N$ . By McDiarmid's inequality [Devroye and Lugosi, 2001, Theorem 2.2], for all  $\varepsilon > 0$ ,

$$\mathbb{P}\left(|\Delta_H - \mathbb{E} \Delta_H| > \varepsilon\right) \leq 2 \exp(-2N\varepsilon^2).$$

To bound  $\mathbb{E} \Delta_H$ , consider the class of sets

$$\mathcal{C} := \left\{ (x, z) : U_\alpha(x) \leq \lambda, z > \tau \mid \lambda \in \Lambda \right\}.$$

Then  $\Delta_H = \sup_{C \in \mathcal{C}} |P_N(C) - P(C)|$ , and by the maximal inequality [Devroye and Lugosi, 2001, Theorem 3.1],

$$\mathbb{E} \Delta_H \leq 2 \sqrt{\frac{\log(2\mathcal{S}(N))}{N}},$$

where  $\mathcal{S}(N)$  is the shatter coefficient of  $\mathcal{C}$ . Fix any sample  $\{(x_i, z_i)\}_{i=1}^N$  and write  $u_i := U_\alpha(x_i)$ . Since  $\tau$  is fixed,

$$\mathbf{1}\{(x_i, z_i) \in \mathcal{C}_\lambda\} = \mathbf{1}\{u_i \leq \lambda\} \mathbf{1}\{z_i > \tau\}.$$

Points with  $z_i \leq \tau$  are always labeled 0, and among points with  $z_i > \tau$  the labeling is determined by a single threshold  $\lambda$  on  $\{u_i\}$ . Hence, as  $\lambda$  varies, the labeling can change only when  $\lambda$  crosses one of the at most  $N$  values  $\{u_i\}_{i=1}^N$ , so at most  $N + 1$  distinct labelings are possible. Therefore  $\mathcal{S}(N) \leq N + 1$ , and

$$\mathbb{E} \Delta_H \leq 2 \sqrt{\frac{\log(2(N+1))}{N}}.$$

Combining with McDiarmid and taking  $\delta_H \in (0, 1)$  yields that with probability at least  $1 - \delta_H$ ,

$$\sup_{\lambda \in \Lambda} |\widehat{H}_N(\lambda) - H(\lambda)| \leq \varepsilon_H := 2 \sqrt{\frac{\log(2(N+1))}{N}} + \sqrt{\frac{\log(2/\delta_H)}{2N}}. \quad (6)$$

**Remark 1** (Sharper uniform deviations). *Using more refined empirical process techniques (e.g., chaining/entropy bounds), one can obtain a DKW-type uniform deviation bound of order*

$$\sup_{\lambda \in \Lambda} |\widehat{H}_N(\lambda) - H(\lambda)| \lesssim \sqrt{\frac{\log(1/\delta_H)}{N}}$$

(up to universal constants), removing the extra  $\sqrt{\log N}$  factor; see, e.g., [Devroye and Lugosi, 2001, Section 3.2]. We keep (6) for simplicity.

**Step 2: DKW uniform deviation for the denominator.** Define  $\Delta_G := \sup_{\lambda \in \Lambda} |\widehat{G}_N(\lambda) - G(\lambda)|$ . Since  $\widehat{G}_N(\lambda)$  is the empirical CDF of the scalar variables  $u_i = U_\alpha(X_i)$ , the Dvoretzky–Kiefer–Wolfowitz [Devroye and Lugosi, 2001, Theorem 3.3] inequality implies that for any  $\delta_G \in (0, 1)$ , with probability at least  $1 - \delta_G$ ,

$$\sup_{\lambda \in \Lambda} |\widehat{G}_N(\lambda) - G(\lambda)| \leq \varepsilon_G := \sqrt{\frac{\log(2/\delta_G)}{2N}}. \quad (7)$$

**Step 3: Uniform ratio bound and choice of  $\lambda^*$ .** Let  $\mathcal{E}_H$  denote the event in (6) and  $\mathcal{E}_G$  the event in (7), i.e.,

$$\mathcal{E}_H := \left\{ \sup_{\lambda \in \Lambda} |\widehat{H}_N(\lambda) - H(\lambda)| \leq \varepsilon_H \right\}, \quad \mathcal{E}_G := \left\{ \sup_{\lambda \in \Lambda} |\widehat{G}_N(\lambda) - G(\lambda)| \leq \varepsilon_G \right\}.$$

Define their intersection

$$\mathcal{E} := \mathcal{E}_H \cap \mathcal{E}_G = \left\{ \sup_{\lambda \in \Lambda} |\widehat{H}_N(\lambda) - H(\lambda)| \leq \varepsilon_H, \sup_{\lambda \in \Lambda} |\widehat{G}_N(\lambda) - G(\lambda)| \leq \varepsilon_G \right\}.$$

By (6) and (7) and a union bound (taking  $\delta_H = \delta_G = \delta/2$ ),

$$\mathbb{P}(\mathcal{E}) \geq 1 - \delta.$$

For  $\lambda \in \Lambda$  with  $\widehat{G}_N(\lambda) > \varepsilon_G$ , define the empirical ratio

$$\bar{q}(\lambda) := \frac{\widehat{H}_N(\lambda) + \varepsilon_H}{\widehat{G}_N(\lambda) - \varepsilon_G}.$$

We now choose  $\lambda$  by enforcing  $\bar{q}(\lambda) \leq \eta$ . Define the feasible set of thresholds

$$\mathcal{F} := \left\{ \lambda \in \Lambda : \widehat{G}_N(\lambda) > \varepsilon_G \text{ and } \bar{q}(\lambda) \leq \eta \right\},$$

and let  $\lambda^* := \max \mathcal{F}$  (with the convention that if  $\mathcal{F} = \emptyset$  then  $A_{\lambda^*, \alpha} = \emptyset$ ). By construction, whenever  $\mathcal{F} \neq \emptyset$  the selected  $\lambda^*$  satisfies  $\widehat{G}_N(\lambda^*) > \varepsilon_G$ .

On the event  $\mathcal{E} = \mathcal{E}_H \cap \mathcal{E}_G$ , we have for all  $\lambda \in \Lambda$  that  $H(\lambda) \leq \widehat{H}_N(\lambda) + \varepsilon_H$  and  $G(\lambda) \geq \widehat{G}_N(\lambda) - \varepsilon_G$ . Applying this at  $\lambda = \lambda^*$  and using  $\widehat{G}_N(\lambda^*) > \varepsilon_G$  yields

$$G(\lambda^*) \geq \widehat{G}_N(\lambda^*) - \varepsilon_G > 0,$$

so  $q(\lambda^*) = H(\lambda^*)/G(\lambda^*)$  is well-defined, and moreover

$$q(\lambda^*) = \frac{H(\lambda^*)}{G(\lambda^*)} \leq \frac{\widehat{H}_N(\lambda^*) + \varepsilon_H}{\widehat{G}_N(\lambda^*) - \varepsilon_G} = \bar{q}(\lambda^*) \leq \eta,$$

where the last inequality holds by the definition of  $\lambda^* \in \mathcal{F}$ .

Finally, since  $\mathcal{E} \subseteq \{q(\lambda^*) \leq \eta\}$ , we conclude that

$$\mathbb{P}(q(\lambda^*) \leq \eta) \geq 1 - \delta.$$

□

**Theorem 6.** *Let  $(X, Z)$  be random variables and let  $U_\alpha : \mathcal{X} \rightarrow \mathbb{R}$  be measurable. Fix  $\tau \in \mathbb{R}$  and define the selection event  $A = \{U_\alpha(X) < \tau\}$ , and assume  $\mathbb{P}(A) > 0$ . If  $U_\alpha$  is conditionally valid at level  $\alpha$ , i.e.*

$$\mathbb{P}(Z > U_\alpha(X) \mid X) \leq \alpha \quad a.s., \tag{8}$$

then  $\mathbb{P}(Z > \tau \mid A) \leq \alpha$ .

*Proof.* On the event  $A$  we have  $U_\alpha(X) < \tau$ , hence  $\{Z > \tau\} \subseteq \{Z > U_\alpha(X)\}$ . Therefore,

$$\mathbb{P}(Z > \tau \mid X)\mathbf{1}_A \leq \mathbb{P}(Z > U_\alpha(X) \mid X)\mathbf{1}_A \leq \alpha\mathbf{1}_A,$$

where the last inequality uses (8). Taking conditional expectation given  $A$  yields

$$\mathbb{P}(Z > \tau \mid A) = \mathbb{E}[\mathbb{P}(Z > \tau \mid X) \mid A] \leq \alpha.$$

□

## G Other tables

Here we present the simulation results for the remaining variants of LOCUS.

Table 4: **Marginal coverage check for Locus.** Reports the coverage probability,  $\mathbb{P}(Z < U_\alpha(x))$ , which is expected to be approximately  $1 - \alpha$ .

Dataset	BART (%)	BART ( $\gamma$ ) (%)	MC Dropout (%)	MC Dropout( $\gamma$ ) (%)
airfoil	89.4 (80.4; 93.1)	90.7 (84.1; 95.4)	88.7 (81.1; 93.4)	91.1 (80.9; 94.8)
bike	90.6 (89.6; 91.4)	91.3 (90.0; 91.9)	91.1 (90.5; 92.2)	92.8 (92.0; 93.6)
concrete	90.8 (84.5; 94.7)	91.3 (84.4; 96.1)	89.3 (84.9; 95.2)	91.7 (83.0; 97.1)
cycle	90.3 (88.5; 91.6)	90.9 (89.4; 92.1)	90.0 (88.5; 91.8)	91.1 (89.3; 92.3)
electric	90.3 (88.8; 92.0)	90.5 (89.2; 92.4)	90.0 (88.1; 91.3)	91.3 (89.8; 92.7)
homes	90.5 (89.0; 91.3)	90.9 (90.0; 91.9)	90.3 (89.2; 91.1)	92.4 (91.1; 93.5)
meps19	89.7 (88.4; 91.1)	92.0 (90.3; 93.0)	89.9 (88.2; 91.3)	90.9 (89.8; 92.8)
protein	89.9 (89.1; 90.6)	90.6 (89.9; 91.6)	89.7 (89.0; 90.7)	91.6 (90.8; 92.2)
star	90.1 (85.9; 92.4)	91.0 (86.4; 95.0)	90.8 (86.1; 93.1)	90.3 (87.1; 94.1)
superconductivity	89.8 (88.3; 90.8)	90.6 (88.8; 91.5)	89.9 (87.8; 90.9)	91.6 (90.1; 92.6)
wec	89.9 (89.3; 90.5)	90.8 (90.0; 91.2)	89.8 (89.4; 90.3)	92.3 (91.6; 93.1)
winered	90.3 (86.5; 95.1)	92.2 (86.5; 96.0)	90.0 (84.9; 95.6)	91.2 (87.2; 96.0)
winewhite	90.2 (88.2; 92.8)	91.1 (89.5; 93.5)	90.3 (87.5; 92.5)	91.4 (89.2; 93.9)

Table 5: **Acceptance rate for (Locus).** Acceptance probability,  $\mathbb{P}(X \in A_\lambda)$  (%), over the test split. LOCUS uses the score  $U_\alpha$  with fixed calibration level  $\alpha = 10\%$ . Entries are the median over 30 runs, with the 5th and 95th percentiles in parentheses.

Dataset	BART (%)	BART ( $\gamma$ ) (%)	MC Dropout (%)	MC Dropout( $\gamma$ ) (%)
airfoil	6.3 (0.0; 26.2)	<b>9.9 (0.7; 23.8)</b>	2.6 (0.0; 13.1)	1.0 (0.0; 23.2)
bike	<b>28.0 (25.3; 29.0)</b>	26.5 (25.2; 28.2)	15.5 (12.5; 19.2)	13.8 (11.8; 16.8)
concrete	<b>0.5 (0.0; 5.8)</b>	0.0 (0.0; 1.9)	0.0 (0.0; 0.0)	0.0 (0.0; 1.0)
cycle	<b>0.0 (0.0; 0.5)</b>	<b>0.0 (0.0; 0.1)</b>	<b>0.0 (0.0; 0.4)</b>	<b>0.0 (0.0; 0.0)</b>
electric	1.8 (0.3; 3.2)	<b>2.8 (1.0; 4.4)</b>	0.7 (0.1; 2.5)	0.3 (0.0; 2.7)
homes	15.8 (12.1; 18.6)	<b>16.1 (12.7; 18.2)</b>	14.0 (9.8; 18.0)	11.7 (9.3; 14.6)
meps19	4.7 (0.3; 8.4)	3.9 (0.3; 19.0)	<b>33.1 (25.0; 39.1)</b>	31.7 (27.2; 37.5)
protein	0.0 (0.0; 0.0)	0.0 (0.0; 0.0)	<b>11.2 (9.4; 12.7)</b>	9.1 (7.4; 11.5)
star	<b>0.0 (0.0; 1.4)</b>	<b>0.0 (0.0; 0.5)</b>	<b>0.0 (0.0; 3.1)</b>	<b>0.0 (0.0; 0.5)</b>
superconductivity	28.3 (25.0; 32.7)	26.5 (22.6; 30.3)	<b>34.6 (31.3; 37.4)</b>	29.2 (26.0; 33.6)
wec	5.3 (3.0; 9.8)	6.7 (2.9; 9.3)	<b>52.9 (50.6; 54.6)</b>	49.8 (47.1; 51.6)
winered	<b>0.0 (0.0; 5.7)</b>	<b>0.0 (0.0; 4.2)</b>	<b>0.0 (0.0; 3.9)</b>	<b>0.0 (0.0; 2.6)</b>
winewhite	<b>0.0 (0.0; 0.3)</b>	<b>0.0 (0.0; 1.1)</b>	<b>0.0 (0.0; 0.4)</b>	<b>0.0 (0.0; 0.2)</b>

Table 6: **Conditional large-loss rate.** Conditional exceedance among accepted points,  $\mathbb{P}(Z > \tau | X \in A_\lambda)$  (%) over the test split. LOCUS uses the score  $U_\alpha$  with fixed calibration level  $\alpha = 10\%$ . Entries are the median over 30 runs, with the 5th and 95th percentiles in parentheses; lower is better. Bold marks the lowest value in each row.

Dataset	BART (%)	BART ( $\gamma$ ) (%)	MC Dropout (%)	MC Dropout( $\gamma$ ) (%)
airfoil	<b>0.0 (0.0; 11.5)</b>	<b>0.0 (0.0; 18.7)</b>	7.1 (0.0; 30.7)	6.9 (0.0; 15.2)
bike	1.6 (0.7; 2.4)	<b>1.0 (0.4; 1.7)</b>	2.2 (0.7; 4.4)	1.9 (0.7; 4.1)
concrete	<b>0.0 (0.0; 65.0)</b>	<b>0.0 (0.0; 50.0)</b>	100.0 (100.0; 100.0)	<b>0.0 (0.0; 90.0)</b>
cycle	33.3 (2.5; 86.7)	100.0 (10.0; 100.0)	<b>0.0 (0.0; 0.0)</b>	– (–; –)
electric	4.2 (0.0; 20.5)	4.8 (0.0; 15.9)	16.7 (0.0; 37.3)	<b>0.0 (0.0; 31.2)</b>
homes	5.0 (3.5; 7.0)	5.6 (3.3; 6.6)	4.9 (2.9; 6.9)	<b>4.0 (2.0; 5.5)</b>
meps19	2.6 (0.0; 6.7)	<b>2.4 (0.0; 7.7)</b>	5.3 (4.0; 6.8)	4.5 (2.9; 6.0)
protein	<b>0.0 (0.0; 0.0)</b>	– (–; –)	3.9 (2.3; 5.2)	2.7 (1.2; 4.2)
star	<b>0.0 (0.0; 80.0)</b>	<b>0.0 (0.0; 0.0)</b>	<b>0.0 (0.0; 60.0)</b>	<b>0.0 (0.0; 100.0)</b>
superconductivity	2.5 (1.4; 3.2)	<b>2.3 (1.2; 3.2)</b>	3.0 (2.0; 4.1)	<b>2.3 (1.0; 3.0)</b>
wec	4.3 (1.7; 8.1)	2.9 (1.6; 7.0)	2.3 (2.0; 3.1)	<b>2.1 (1.7; 2.7)</b>
winered	10.0 (0.0; 80.0)	<b>0.0 (0.0; 77.8)</b>	<b>0.0 (0.0; 69.4)</b>	<b>0.0 (0.0; 0.0)</b>
winewhite	<b>0.0 (0.0; 28.3)</b>	<b>0.0 (0.0; 14.6)</b>	<b>0.0 (0.0; 68.1)</b>	<b>0.0 (0.0; 90.0)</b>

Table 7: **Tuned acceptance rate at matched target coverage (Locus-Tuned).** Acceptance probability,  $\mathbb{P}(X \in A_\lambda)$  (%). For each dataset and method, the threshold  $\lambda$  is selected on the validation split to target an acceptance rate of  $\approx 70\%$ ; test performance is then reported. LOCUS-TUNED methods use the LOCUS score  $U_\alpha$  with fixed calibration level  $\alpha = 10\%$ . Entries are the median over 30 runs, with the 5th and 95th percentiles in parentheses.

Dataset	Baselines (no Locus)		Locus-Tuned (loss-quantile score)			
	IFlag	VARNet	Locus-BART	Locus-BART ( $\gamma$ )	Locus-MC	Locus-MC ( $\gamma$ )
airfoil	73.2 (63.8; 80.8)	<b>82.8 (69.1; 95.9)</b>	72.8 (65.1; 78.8)	71.2 (61.5; 78.9)	70.5 (61.2; 77.2)	71.5 (62.5; 77.2)
bike	73.0 (73.0; 73.0)	<b>88.2 (74.8; 94.3)</b>	72.2 (70.9; 74.6)	71.9 (70.5; 74.3)	73.3 (71.9; 75.1)	72.5 (71.0; 73.7)
concrete	72.3 (66.0; 80.1)	<b>80.6 (73.8; 89.9)</b>	72.3 (61.6; 83.2)	72.3 (61.0; 85.9)	72.8 (64.5; 86.1)	74.3 (64.1; 80.7)
cycle	72.4 (67.9; 76.2)	<b>92.2 (74.8; 98.9)</b>	73.8 (69.2; 78.6)	73.1 (68.4; 78.9)	75.0 (70.8; 81.9)	74.0 (68.8; 80.5)
electric	71.5 (67.5; 75.9)	<b>79.0 (71.5; 83.9)</b>	71.7 (68.6; 74.9)	71.5 (69.1; 75.4)	71.0 (68.2; 74.7)	71.4 (69.1; 75.1)
homes	71.9 (69.6; 74.3)	<b>80.8 (72.4; 88.1)</b>	71.3 (69.3; 73.1)	71.3 (69.4; 73.5)	71.3 (69.2; 73.7)	70.8 (68.5; 73.1)
meps19	71.7 (69.5; 74.5)	<b>79.4 (68.5; 84.8)</b>	73.1 (69.3; 76.1)	72.3 (69.7; 75.5)	71.3 (68.8; 73.4)	71.3 (68.8; 74.0)
protein	72.3 (70.0; 74.5)	<b>73.1 (71.3; 79.2)</b>	71.1 (69.0; 73.7)	71.1 (69.6; 74.0)	71.2 (68.7; 72.7)	71.2 (69.9; 73.2)
star	72.8 (63.9; 79.3)	73.0 (65.2; 80.5)	<b>76.3 (67.0; 84.4)</b>	75.1 (66.4; 83.5)	73.5 (66.4; 77.3)	74.7 (65.7; 81.4)
superconductivity	71.5 (69.7; 74.0)	<b>82.4 (71.6; 88.8)</b>	70.9 (69.3; 73.6)	71.2 (69.2; 72.5)	71.4 (69.2; 75.0)	71.4 (68.6; 73.9)
wec	71.6 (69.7; 74.0)	<b>88.1 (85.2; 89.7)</b>	71.2 (69.6; 72.8)	71.1 (69.4; 72.2)	70.6 (69.0; 72.5)	70.3 (69.1; 72.1)
winered	70.9 (62.1; 77.6)	<b>73.4 (65.0; 80.6)</b>	70.9 (63.1; 79.4)	67.5 (59.0; 78.9)	73.1 (62.6; 76.9)	71.6 (61.7; 81.2)
winewhite	72.9 (68.1; 76.4)	72.7 (66.2; 79.4)	<b>80.2 (69.9; 85.2)</b>	77.1 (68.6; 81.9)	76.5 (69.7; 83.8)	76.3 (69.8; 82.6)

Table 8: **Tuned acceptance rate at matched target coverage (Locus- $\alpha$ ).** Acceptance probability,  $\mathbb{P}(X \in A_\lambda)$  (%). For each dataset and method, the threshold  $\lambda$  is selected on the validation split to target an acceptance rate of  $\approx 70\%$ ; test performance is then reported. LOCUS- $\alpha$  methods use the LOCUS score  $U_\alpha$  with fixed calibration level  $\alpha = 10\%$ . Entries are the median over 30 runs, with the 5th and 95th percentiles in parentheses.

Dataset	Baselines (no Locus)		Locus- $\alpha$ (loss-quantile score)			
	IFlag	VARNet	Locus-BART	Locus-BART ( $\gamma$ )	Locus-MC	Locus-MC ( $\gamma$ )
airfoil	73.2 (63.8; 80.8)	<b>82.8 (69.1; 95.9)</b>	71.5 (64.5; 78.1)	71.5 (62.5; 79.2)	70.5 (60.3; 77.5)	71.5 (63.5; 82.3)
bike	73.0 (73.0; 73.0)	<b>88.2 (74.8; 94.3)</b>	71.4 (69.5; 73.3)	71.7 (70.3; 73.6)	72.3 (70.9; 74.0)	70.9 (69.2; 72.8)
concrete	72.3 (66.0; 80.1)	<b>80.6 (73.8; 89.9)</b>	71.8 (62.4; 83.7)	71.8 (62.5; 84.2)	73.8 (62.0; 83.6)	72.8 (64.5; 79.2)
cycle	72.4 (67.9; 76.2)	<b>92.2 (74.8; 98.9)</b>	71.6 (68.5; 75.1)	71.6 (67.4; 75.8)	72.6 (68.2; 79.1)	75.8 (68.8; 85.3)
electric	71.5 (67.5; 75.9)	<b>79.0 (71.5; 83.9)</b>	71.6 (68.2; 74.2)	70.8 (67.8; 73.4)	71.0 (67.7; 74.0)	71.1 (68.5; 75.2)
homes	71.9 (69.6; 74.3)	<b>80.8 (72.4; 88.1)</b>	71.6 (68.6; 72.9)	70.5 (68.8; 73.5)	70.9 (68.5; 73.5)	70.7 (68.9; 72.8)
meps19	71.7 (69.5; 74.5)	<b>79.4 (68.5; 84.8)</b>	71.1 (67.2; 72.3)	70.4 (68.5; 72.3)	70.0 (68.0; 72.0)	70.2 (67.5; 71.9)
protein	72.3 (70.0; 74.5)	<b>73.1 (71.3; 79.2)</b>	<b>73.1 (69.9; 76.5)</b>	72.1 (70.5; 74.4)	71.2 (69.5; 72.7)	71.6 (69.2; 74.0)
star	72.8 (63.9; 79.3)	73.0 (65.2; 80.5)	<b>75.1 (66.6; 83.3)</b>	73.5 (64.2; 80.6)	73.5 (66.7; 81.2)	72.6 (67.3; 79.6)
superconductivity	71.5 (69.7; 74.0)	<b>82.4 (71.6; 88.8)</b>	70.9 (68.9; 72.8)	70.8 (68.6; 72.8)	71.9 (69.2; 73.3)	71.1 (69.3; 73.3)
wec	71.6 (69.7; 74.0)	<b>88.1 (85.2; 89.7)</b>	70.6 (69.2; 72.0)	70.1 (68.9; 72.0)	70.1 (68.5; 71.5)	70.3 (69.0; 71.3)
winered	70.9 (62.1; 77.6)	73.4 (65.0; 80.6)	<b>74.4 (62.8; 80.1)</b>	71.9 (61.3; 80.7)	74.1 (60.8; 80.3)	71.9 (62.8; 81.7)
winewhite	72.9 (68.1; 76.4)	72.7 (66.2; 79.4)	<b>75.1 (67.1; 78.0)</b>	73.7 (67.4; 77.9)	72.3 (65.5; 79.4)	73.0 (67.6; 77.2)

Table 9: **Tuned conditional large-loss rate at matched acceptance (Locus- $\alpha$ )**. Conditional exceedance among accepted points,  $\mathbb{P}(Z > \tau \mid X \in A_\lambda)$  (%). For each dataset and method, the threshold  $\lambda$  is selected on the validation split to achieve an acceptance rate of  $\approx 70\%$ ; test performance is then reported. LOCUS- $\alpha$  methods use the LOCUS score  $U_\alpha$  with fixed calibration level  $\alpha = 10\%$ . Entries are the median over 30 runs, with the 5th and 95th percentiles in parentheses; lower is better. Bold marks the lowest value in each row.

Dataset	Baselines (no Locus)		Locus- $\alpha$ (loss-quantile score)			
	IFlag	VARNet	Locus-BART	Locus-BART ( $\gamma$ )	Locus-MC	Locus-MC ( $\gamma$ )
airfoil	31.0 (27.4; 35.3)	27.5 (23.0; 30.7)	23.3 (19.6; 26.7)	<b>22.2 (18.4; 28.3)</b>	24.5 (19.2; 29.3)	24.7 (19.1; 27.4)
bike	30.1 (30.1; 30.1)	28.4 (26.1; 29.2)	<b>19.0 (18.3; 20.8)</b>	19.4 (18.3; 20.6)	22.1 (21.3; 22.7)	21.8 (20.6; 23.1)
concrete	33.5 (27.2; 38.6)	27.7 (23.0; 31.2)	<b>23.7 (19.0; 28.0)</b>	25.2 (20.1; 29.1)	27.6 (20.0; 31.9)	27.4 (21.8; 32.9)
cycle	28.9 (27.2; 30.0)	29.7 (28.5; 30.2)	<b>26.7 (25.2; 27.8)</b>	27.1 (25.5; 28.2)	28.4 (26.7; 29.6)	28.9 (27.5; 30.1)
electric	31.5 (30.1; 32.1)	29.4 (28.1; 30.7)	<b>24.1 (22.2; 25.4)</b>	<b>24.1 (22.4; 25.8)</b>	24.7 (22.9; 26.0)	24.6 (23.2; 26.4)
homes	34.8 (33.7; 36.0)	26.6 (24.8; 27.7)	19.2 (17.9; 20.1)	19.3 (17.7; 20.6)	19.0 (17.6; 20.2)	<b>18.9 (18.1; 20.0)</b>
meps19	36.4 (35.4; 37.4)	24.8 (21.5; 26.6)	14.0 (12.3; 15.0)	13.8 (11.9; 14.5)	<b>13.0 (11.7; 14.3)</b>	<b>13.0 (11.9; 14.4)</b>
protein	28.0 (27.4; 29.0)	27.4 (25.8; 29.4)	24.6 (23.5; 25.2)	23.8 (22.9; 25.2)	22.8 (21.4; 23.5)	<b>22.6 (21.9; 23.5)</b>
star	29.1 (26.3; 31.9)	29.0 (26.9; 33.8)	29.1 (26.1; 31.9)	29.3 (26.1; 32.4)	<b>28.5 (25.6; 31.5)</b>	28.9 (26.5; 33.1)
superconductivity	24.0 (23.1; 25.3)	25.8 (21.3; 28.1)	<b>17.9 (17.0; 19.0)</b>	18.1 (16.4; 19.2)	18.3 (16.7; 19.7)	<b>17.9 (16.7; 19.3)</b>
wec	34.8 (33.5; 35.3)	23.0 (21.4; 24.6)	15.1 (12.2; 18.4)	14.6 (12.9; 18.7)	<b>8.2 (7.0; 9.2)</b>	<b>8.2 (7.4; 8.9)</b>
winered	30.2 (26.6; 32.9)	28.8 (24.9; 32.9)	27.5 (24.0; 30.7)	<b>26.9 (23.3; 29.3)</b>	27.5 (23.4; 30.5)	27.5 (23.1; 31.5)
winewhite	29.9 (28.2; 31.5)	30.3 (28.3; 31.7)	27.1 (24.6; 29.3)	<b>26.5 (24.3; 29.3)</b>	27.8 (24.1; 29.4)	27.4 (25.0; 29.2)